



## 上海交通大学学位论文

# 铆接过程中振动引起的测量不准确性分析

姓 名： 朱敬田，王一鸣, Mansur Ayazbayev,

赵恒, 高语嘉

学 号： 519021911096, 519370910080,

519370990010, 520021911230,

520370910045

导 师： 黄佩森

学 院： 密西根学院

专业名称： 电子与计算机工程, 机械工程,

材料科学与工程

申请学位层次： 学士

2024 年 08 月

**A Dissertation Submitted to  
Shanghai Jiao Tong University for Bachelor's Degree**

**ANALYSIS OF VIBRATION-INDUCED  
MEASUREMENT INACCURACIES IN RIVETING  
PROCESSES**

**Author: Zhu Jingtian, Wang Yiming,  
Ayazbayev Mansur, Zhao Heng, Gao Yujia  
Supervisor: Huang Peisen**

**UM-SJTU Joint Institute  
Shanghai Jiao Tong University  
Shanghai, P.R. China**

**August, 2024**

## 上海交通大学

## 学位论文原创性声明

本人郑重声明：所呈交的学位论文，是本人在导师的指导下，独立进行研究工作所取得的成果。除文中已经注明引用的内容外，本论文不包含任何其他个人或集体已经发表或撰写过的作品成果。对本文的研究做出重要贡献的个人和集体，均已在文中以明确方式标明。本人完全知晓本声明的法律后果由本人承担。

赵恒,高语嘉

学位论文作者签名：朱鹤园,王一鸣, foydach

日期：2024年08月06日

## 上海交通大学

## 学位论文使用授权书

本人同意学校保留并向国家有关部门或机构送交论文的复印件和电子版，允许论文被查阅和借阅。

本学位论文属于：

公开论文

内部论文，保密  1 年 /  2 年 /  3 年，过保密期后适用本授权书。

秘密论文，保密 \_\_\_\_ 年（不超过 10 年），过保密期后适用本授权书。

机密论文，保密 \_\_\_\_ 年（不超过 20 年），过保密期后适用本授权书。

（请在以上方框内选择打“√”）

foydach, 赵恒, 高语嘉

学位论文作者签名：朱鹤园,王一鸣

日期：2024 年 08 月 06 日

指导教师签名：陈晓华

日期：2024 年 08 月 06 日

## 摘要

本项目由上海希腾电子信息技术有限责任公司赞助，旨在解决公司在制造过程中因铆钉振动引起误差，从而导致其产品未能满足客户要求的问题。项目以开发一个可以捕捉和分析铆接过程中产生的振动的系统为目标，并基于实验结果提出减少振动幅度的方案。根据公司对精确振动检测与可视化的要求，我们确定了包括系统质量、体积、价格、处理时间、准确率，传感器的分辨率、重复性、响应时间、频率响应范围和误差范围在内的工程规格。从结构上来说，我们的系统由硬件和软件两部分组成。硬件包括基恩士位移激光传感器、放大器和 Arduino 控制板；软件使用了 Python 语言的 PyQt 框架构建。硬件设备通过捕捉原始数据并将其转化成数字信号发送到计算机，从而实现软件中对振动模型的可视化和异常识别。搭建这一系统的总成本为人民币 1004 元。以上所提及的元件和设备选择均基于预算限制和工程规格要求。实验结果表明，我们的产品除了系统在检测振动幅度和频率方面的成功率低于预期外，在所有其他规格上均达到了目标值。由于我们在选择硬件时还不了解铆接过程中确切的震动范围，因此所选硬件可检测到的最小差异与实际需求相比仍过大，限制了系统在较小振动情况下的检测能力。目前，我们的系统仅能在检测大振动时达到预期的成功率。因此，未来我们将使用更精确的微控制器以提高检测精度。通过实际实验，我们发现振动幅度显著受 U 形部件的宽度和铆接输入压力的影响，而峰值振动频率则不受这些因素的影响。我们希望本项目能帮助上海希腾电子信息技术有限责任公司更有效地控制铆接过程，节省时间和能源，并提高其市场竞争力。

**关键词：**振动分析；铆接准确性；数据可视化

## ABSTRACT

This project, sponsored by *Shanghai Systence*, addresses inaccuracies caused by rivet vibrations during manufacturing, which have prevented their products from meeting client requirements. The project aims to develop a cost-effective system to capture and analyze these vibrations and provide recommendations to mitigate them. To fit the company's specific requirements on accurate visualization and analysis of vibrations, we have identified engineering specifications including mass, volume, price, system processing time, sensor resolution, repeatability, response time, frequency response range, error range, and success rate. Our system consists of a hardware set, which includes a *Keyence* displacement laser sensor, an amplifier, and an Arduino board, as well as a software interface built using PyQt in Python; hardware captures raw data and sends digital signals to computer for visualizing vibration patterns and identifying anomalies. The total cost was RMB 1004. All concepts were chosen based on budget limit and meeting specifications. Validation results indicate that our product meets the target values across all specifications, except for the system's success rate in detecting vibration amplitude and frequencies. Currently, our system achieves the desired success rate only when detecting conditions with large vibrations. However, in cases of small vibrations, the hardware we selected limits detection capabilities due to its minimum detectable difference. This limitation arose because we were unaware of the exact vibration extent in the riveting process when choosing the hardware. Consequently, future work will involve using a more precise microcontroller for higher accuracy. Through actual experiments, we found that vibration amplitude is significantly affected by the width of the U-shaped part and the input pressure for riveting, while the peak vibration frequency remains unaffected by these factors. We hope this project will help Shanghai Systence control the riveting process more effectively, saving time and energy, and enhancing their market competitiveness.

**Key words:** vibration analysis; rivet accuracy; data visualization

## Contents

<b>摘要 .....</b>	<b>I</b>
<b>ABSTRACT .....</b>	<b>II</b>
<b>Chapter 1 Introduction .....</b>	<b>1</b>
1.1 Project Background .....	1
1.2 Problem.....	1
1.3 Benchmarks .....	3
1.3.1 TURCK - Model: CMVT-QR20-IOLX3-H1141.....	3
1.3.2 FLUKE 820-2 LED Stroboscope .....	4
1.3.3 enDAQ S3 Vibration Sensor.....	4
1.4 Literature on Vibration Sensing and Analysis .....	5
1.4.1 Sensors: Data Collection .....	5
1.4.2 Vibration Theory .....	6
1.4.3 Data Analysis.....	7
<b>Chapter 2 Design Specifications .....</b>	<b>9</b>
2.1 Customer Requirements .....	9
2.2 Engineering Specifications .....	10
<b>Chapter 3 Concept Generation and Selection .....</b>	<b>12</b>
3.1 Concept Morphological Analysis .....	12
3.2 Concept Evaluation .....	12
3.2.1 Sensor Selection .....	12
3.2.2 Micro-controller Selection .....	14
3.2.3 Analysis Tool Selection .....	15
3.2.4 User Interface Framework Selection .....	15
3.3 Concept Description .....	17
<b>Chapter 4 Final Product Design .....</b>	<b>19</b>

4.1	Final Design Overview .....	19
4.2	Detailed Designs .....	20
4.2.1	U-shaped Part .....	20
4.2.2	Data Collection Hardware Set .....	22
4.2.3	User Interface .....	24
4.2.4	Modeling and Simulation .....	25
<b>Chapter 5 Manufacture and Validation Results .....</b>		<b>28</b>
5.1	Manufacturing Plan .....	28
5.1.1	U-shaped Part .....	28
5.1.2	Hardware Connection and Encapsulation .....	28
5.1.3	User Interface .....	29
5.1.4	Modeling and Simulation .....	30
5.2	Validation.....	33
5.2.1	Validation Results .....	33
5.2.2	Engineering Specification Analysis .....	36
5.3	Engineering Changes Notice .....	37
<b>Chapter 6 Findings and Discussion.....</b>		<b>39</b>
6.1	Findings .....	39
6.2	Discussion .....	40
6.2.1	Hardware Limitation .....	40
6.2.2	Ansys Simulation .....	42
6.3	Future works .....	43
<b>Chapter 7 Conclusion.....</b>		<b>45</b>
<b>Acknowledgements .....</b>		<b>47</b>
<b>Appendix 1: Author Bios.....</b>		<b>48</b>
<b>Appendix 2: Bill of Materials .....</b>		<b>51</b>
<b>Appendix 3: ECN and Relevant Figures and Codes .....</b>		<b>52</b>

3.1	Engineering Change Notice .....	52
3.2	Validation Plots for Developed System .....	52
3.3	Code .....	55

# Chapter 1 Introduction

## 1.1 Project Background

*Shanghai Systence Co.* is a prominent entity in the assembly line industry, specializing in the production of three primary product categories: electro-mechanical assembly presses, riveting machines (Illustration 1–1(a)), and the comprehensive design and construction of assembly line systems for various factories. In this project, we will focus on the optimization of riveting technology, specifically targeting the identification and mitigation of vibration-related issues inherent in the riveting process. The aim is to provide *Shanghai Systence Co.* with actionable insights and recommendations to enhance the efficiency and reliability of their riveting operations. Our investigation is specifically concentrated on radial riveting technology (Illustration 1–1(b)), a widely utilized technique in the assembly of mechanical components. Despite its prevalent use, *Shanghai Systence Co.* faces challenges in quantitatively analyzing the riveting process. The existing methodology predominantly relies on experiential knowledge and qualitative assessments of the rivet's behavior. While this traditional approach has its merits, it often falls short in addressing the nuanced complexities of the riveting process, leading to sub-optimal solutions that result in financial losses, wasted time, and diminished confidence in the company's problem-solving capabilities.

## 1.2 Problem

A thorough literature search on the impact of vibrations during the riveting process on rivet accuracy yielded no substantial results from academic search engines. Consequently, the nature of this problem is primarily based on descriptions provided by *Shanghai Systence Co.* and an example of a previously encountered issue. *Shanghai Systence*, along with their partner *FMW Friedrich*, an industry pioneer in data-driven riveting, report that vibrations are a significant cause of inaccuracies in the riveting process, sometimes failing to meet customer specifications. The riveting process at *Shanghai Systence* involves the machine initially determining the rivet's height before proceeding with the riveting operation until the required height is achieved. However, rivets' vibrating during this process compromise the accuracy

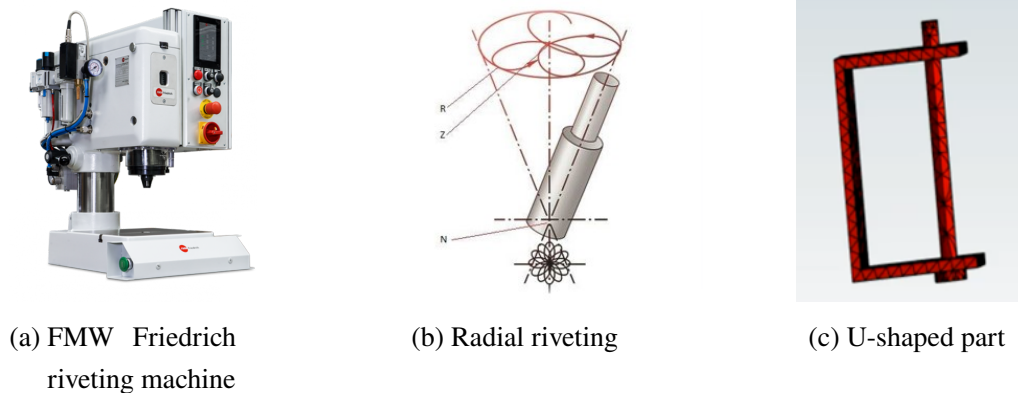


**Illustration 1–1 (a) Riveting machine used in this project<sup>[1]</sup>. (b) The plum petal-shaped pattern for rivet head during radial riveting process<sup>[2]</sup>. (c) SolidWorks modeled U-shaped part.**

of height measurements, resulting in inconsistent output parameters. A notable instance illustrating this issue involved a complex U-shaped riveting part shown in Illustration 1–1(c), where additional bending occurred due to momentum. This complication led to significant time and financial investments as parts were sent to Germany for testing, in-house experiments were conducted, and repeated consultations with the multinational client were necessary. This iterative and inefficient problem-solving approach highlights the urgent need for a quantifiable solution to address the vibration-induced inaccuracies in the riveting process. Therefore, our group aims to address this critical issue by developing a system to quantify and visualize vibrations during the riveting process. The primary objectives include:

- Data Collection: Finding robust sensors to gather real-time data on vibrations occurring during the riveting process.
- Data Visualization: Creating visualization tools to identify anomalies and patterns in the vibration data, providing insights into the correlation between vibrations and rivet accuracy.
- Problem Mitigation: Offering actionable recommendations to eliminate or minimize the impact of vibrations on the riveting process.

By quantifying the impact of vibrations and visualizing the data, group 24 intends to facilitate a deeper understanding of the riveting process anomalies. This approach aims to significantly expedite and economize the problem-solving process for future riveting challenges, thereby enhancing the operational efficiency and product quality for *Shanghai Systence Co.* and its partners.

## 1.3 Benchmarks

### 1.3.1 TURCK - Model: CMVT-QR20-IOLX3-H1141

This vibration and temperature sensor shown in Illustration 1–2(a) is used mainly for the condition monitoring of the equipment. The device features a magnetic surface, which simplifies the attachment process to any metal equipment. Once attached, it is linked with the software that collects the data and can either visualize it for the manual check or automatically notify the responsible engineer if anomalies are detected. One key parameter tracked is the sensor's displacement to monitor vibration states. Weighing 85 grams<sup>[3]</sup>, the sensor is considered relatively lightweight. However, while its size is suitable to put on the riveting machine, it's too large for precise placement on the riveting parts, which are our group's primary interest as in the riveting process, inaccuracies mainly stem from the mechanics of this part rather than the machine failure. Additionally, the product is relatively expensive at 3700 RMB, considering its limitation to equipment monitoring. Nevertheless, the concept of this product is similar to the final outcome that group 24 wants to achieve, though it cannot directly and accurately solve the company's problem.

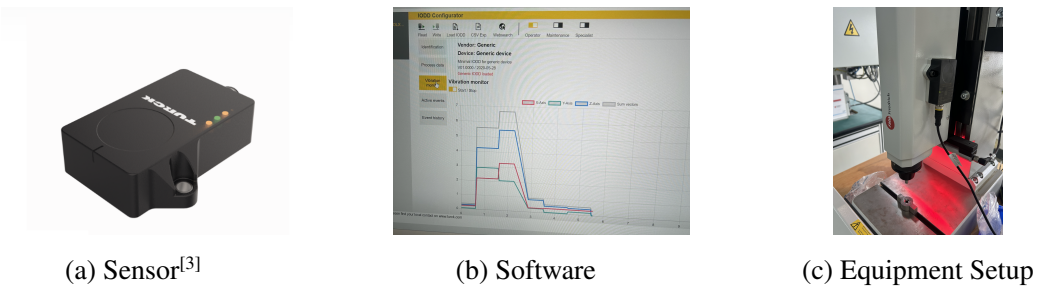


**Illustration 1–2 TURCK - Vibrations and Temperature Control System.** (a) Sensor - measures the connected item's temperature, acceleration, and velocity. (b) The software interface that is used for data visualization, allowing manual analysis of the operation state and can automatically notify the responsible person about the anomalies. (c) is how this equipment is set up on the riveting machine using a magnetic surface.

### 1.3.2 FLUKE 820-2 LED Stroboscope

This product, shown in Illustration 1–3(a), developed by *Fluke*, is designed to detect the running speed of rotating equipment. It can diagnose parasitic oscillations, slippage, or unwanted distortions without being physically attached to the measured part. Although

lightweight at  $0.24\text{kg}$ , its size ( $5.71\text{cm} \times 6.09\text{cm} \times 19.05\text{cm}$ ) make it difficult to place around the rivet. Additionally, it costs  $\$1,923.99^{[4]}$ , which exceeds our budget. Furthermore, it is not easy to be accustomed or adapted to *Shanghai Systene*'s riveting machine, since its hardware and software are already integrated. However, it has several useful features that our group can learn from, including digital pulse width modulation for exceptionally sharp images at high speeds and a quartz-accuracy control system for high precision ( $0.02\% \pm 0.001$ ).



**Illustration 1–3** (a) Fluke vibration sensor. It can quickly record the vibration object and finish analysis on multiple aspects. (b) enDAQ System. The sensor can continuously catch fatal vibration parameters with outside environment conditions for more than 13 hours at a time without charging. (c) The enDAQ analyzing software. It can be imported with data gathered from the sensor and perform corresponding analysis.

### 1.3.3 enDAQ S3 Vibration Sensor

*enDAQ* is a professional company specializing in vibration analysis. It provides paid services for hardware configuration (Illustration 1–3(b)) and free software analysis (Illustration 1–3(c)). The enDAQ S3 Vibration Sensor can function as a general-purpose vibration recorder, with additional environmental sensors. The compact product measures  $76.2\text{mm} \times 29.8\text{mm} \times 15.0\text{mm}$  and weighs only  $40\text{g}$ , and it comes with dust protection. It can operate continuously for 13 hours at its highest sample rate (3200Hz), incorporating many additional embedded sensors into a single system. Its bandwidth ranges from 0 to 300 Hz with  $\pm 5\%$  accuracy. It costs over  $\$1299$  with free and customizable software solutions like *enDAQ LAB* and *enDAQ Cloud*, which support both simple real-time response and complex post analysis<sup>[5]</sup>.

Similar to TRUCK and FLUKE, this system is well-developed and could potentially achieve Team 24's objectives. However, since we have not yet determined the type of vi-

bration occurring on the rivet during the riveting process, it's possible that the vibration may exceed the sensor's bandwidth. Additionally, the enDAQ sensor is quite expensive.

## 1.4 Literature on Vibration Sensing and Analysis

In addition to analyzing competitor products, we reviewed literature related to the three main steps of our project: gathering vibration data through sensors, conducting theoretical vibration analysis, and performing data analysis using software.

### 1.4.1 Sensors: Data Collection

In recent years, significant advancements have been made in the field of vibration data collection through the development of innovative sensor technologies and methodologies. Works by Garcia et al.<sup>[6]</sup>, Liu et al.<sup>[7]</sup>, and Weng et al.<sup>[8]</sup> focus on *Fiber-Optic-Based Vibration Sensors*. These studies explore various applications of fiber-optic technology in vibration measurement, emphasizing its high sensitivity, immunity to electromagnetic interference, and suitability for long-distance monitoring. On the other hand, works by Shukla et al.<sup>[9]</sup> and Guo et al.<sup>[10]</sup> focus on *Smart and Non-Contact Vibration Sensors*. These studies introduce innovative approaches using smart sensors and non-contact methods, leveraging advanced data analysis techniques and deep learning to enhance the efficiency and applicability of vibration measurement systems.

Shukla et al.<sup>[9]</sup> introduce a smart sensor-based monitoring system for real-time vibration measurement and bearing fault detection, employing advanced sensors and data analysis to prevent machinery breakdowns and reduce maintenance costs. Liu et al.<sup>[7]</sup> explore distributed fiber-optic sensors for high-resolution, long-distance vibration detection, enhancing structural health monitoring for large structures like bridges and pipelines by detecting even minor vibrations. Guo et al.<sup>[10]</sup> propose a non-contact vibration sensor using deep learning and image processing, utilizing optical flow for signal extraction and addressing the deployment challenges of traditional sensors, making it suitable for inaccessible or hazardous areas.

Despite their innovative approaches, these papers have certain limitations. The smart sensor-based system, while highly effective for bearing fault detection, is somewhat limited to specific types of machinery and relies on predefined fault patterns, reducing its adaptability to new or unforeseen types of faults. The distributed fiber-optic sensors, though excellent

for large-scale applications, face challenges in terms of installation complexity and cost, and their performance can be affected by environmental conditions such as temperature variations and physical damages to the fiber. The non-contact vibration sensor, despite its advanced capabilities, is susceptible to variations in lighting conditions and background features, which can affect its accuracy, and the need for high computational power for deep learning algorithms might limit its real-time application in certain scenarios. Our data collection efforts will aim to overcome these limitations by focusing on adaptable, cost-effective, and robust solutions for a variety of environmental conditions and applications.

#### 1.4.2 Vibration Theory

In Krodkiewski<sup>[11]</sup>'s book, vibration is defined as the oscillatory motion of a mechanical system about its equilibrium position. Mechanical vibrations can be categorized in various ways. In our project, we aim to discover methods to mitigate vibrations. Therefore, we will classify vibrations based on their causes, which include free vibration, forced vibration, self-excited vibration, and parametric vibration.

Free vibration refers to the vibration that occurs near the equilibrium position after the initial disturbance and no other excitation. The period and frequency of free vibration are determined by the characteristics of the system itself. When considering the effects of resistance, free vibration can be further categorized into underdamped vibration, overdamped vibration, and critically damped vibration, which implies that the period and amplitude of free vibration will be influenced by the magnitude of damping.

Forced vibration occurs when a system is subjected to periodic external forces. It initially manifests as a combination of two vibration states: one determined by the system's natural frequency and the other by the frequency of the driving force. When the driving force is small, the attenuation of free vibration is gradual. Conversely, when the driving force is large, the free vibration decays rapidly. If the frequency of the driving force is close to the natural frequency, the system will exhibit a resonance phenomenon, resulting in larger amplitude vibrations.

Self-excited vibration refers to the phenomenon where a system, after experiencing an initial accidental disturbance, continues to vibrate without the need for external excitation. This sustained vibration occurs at or near the system's natural frequency and does not attenuate

over time. Unlike the previous two types of vibration, the study of self-excited vibration does not focus on the magnitude or form of the disturbance. Instead, it emphasizes the inherent instability of the system itself.

Parametric vibration refers to the phenomenon where the parameters of a vibration system vary periodically due to external forces. Taking the swing as an example, if you want to swing up, people should periodically apply force, swing amplitude, frequency should also change accordingly, the mathematical model describing the parameter vibration is the ordinary differential equation with periodic variable coefficient.

The above analysis provides an overview of the four vibration modes without delving into specific modeling derivations. Once we have identified the vibration type in our project, we can proceed with a more detailed analysis by employing specific research methods that are relevant to that particular type of vibration. This will allow us to gain a deeper understanding of the phenomenon and make informed decisions based on our findings.

### 1.4.3 Data Analysis

The field of vibration data analysis has seen significant advancements, with numerous studies exploring various methods to improve machine monitoring and fault diagnosis. Mohd Ghazali<sup>[12]</sup> provides a systematic review and general overview of vibration analysis techniques. Yan and Gao<sup>[13]</sup>, Staszewski<sup>[14]</sup>, and Saruhan<sup>[15]</sup> focus on specific techniques for vibration analysis. Amihai<sup>[16]</sup> and Zhao<sup>[17]</sup> explore the application of machine learning and artificial intelligence in vibration analysis. Prudhom<sup>[18]</sup> and Jung<sup>[19]</sup> present case studies and practical implementations. Trendafilova<sup>[20]</sup> and Grasso<sup>[21]</sup> introduce innovative methods and frameworks.

Yan and Gao<sup>[13]</sup> proposed the use of the Hilbert-Huang Transform (HHT) for vibration signal analysis, which effectively decomposes nonlinear and non-stationary signals into intrinsic mode functions. This method addresses the limitation of traditional Fourier-based methods in handling non-stationary signals. Staszewski<sup>[14]</sup> introduced a wavelet-based approach for compressing and selecting features from vibration signals. The wavelet transform allows for multi-resolution analysis, making it suitable for detecting transient features. Amihai et al.<sup>[16]</sup> conducted an industrial case study using machine learning to predict asset health based on vibration data. The study employed Random Forest algorithms to predict failures

up to seven days in advance, outperforming traditional persistence techniques. Trendafilova et al.<sup>[20]</sup> developed a method combining Principal Component Analysis (PCA) and pattern recognition for damage detection in an aircraft wing model. This approach reduces the dimensionality of vibration data and enhances damage feature extraction.

While significant advancements have been made in vibration analysis for machine monitoring and diagnosis, several limitations remain. These include computational complexity, sensitivity to noise, dependency on data quality, and the need for extensive historical data. Addressing these limitations is essential for improving the robustness and applicability of these methods in real-world scenarios. Our work will focus on developing robust, scalable methods to collect data related to vibrations during the riveting process, create algorithms that identify anomaly patterns, and suggest solutions. This research aims to enhance the accuracy and reliability of vibration-based fault detection systems, making them more applicable to diverse industrial environments.

## Chapter 2 Design Specifications

### 2.1 Customer Requirements

Our sponsored company, *Shanghai Systence* is the primary customer for this project, as they will be the main users of the product. We collaborated with the company to identify the top 10 customer requirements, summarized in Table 2–1. They are arranged according to their weighted importance.

**Table 2–1 Customer requirements with weighted importance**

Requirements	Weight (1-10)
Accurate vibration capture	10
Easy-to-use	9
Stable (long-distance transport)	9
Accurate vibration analysis	8
Fast	8
Portable	8
Easy-to-install	4
Cheap	3
Less parts needed	2
Appealing design	2

Through discussions with the company, we found that they prioritized accuracy and ease of use over cost and aesthetics of the final product. The highest priority was **accurate vibration capture**, as the company was aware of the existence and impacts of vibrations but needed a way to visualize and categorize them. Therefore, our primary goal was to first obtain the correct vibrations so as to provide further accurate analysis. "**Ease-of-use**" followed, as the product interface needs to be intuitive for engineers. **Stability** refers to the product's durability during long-distance transportation; the final product should maintain good functionality after being transported, as it will be used in various factories and client locations. **Accurate vibration analysis** and **speed (fast)** in both data capture and software processing were also crucial. Additionally, **Portability** and "**Less parts needed**" both means the product should be a compact design that ensures the ease of transport and assembly. **Easy**

**installation** of both software and sensors, though less critical, was still a consideration. The least important factors were **cheap** and **design appeal**, but the company expressed their wish for a good-looking product so that they can also present it in front of their clients.

## 2.2 Engineering Specifications

Based on customer requirements, we established corresponding engineering specifications, summarized in the QFD chart in Illustration 2–1. We categorized those specifications into three main areas: data collection components, data analysis (user interface, software), and overall product attributes. Each category aligns with specific customer requirements. For the overall product, we focused on **mass**, **volume**, and **price**, which correspond to requirements for stability, portability, ease of installation, and minimal components. In terms of the software, we prioritized **processing time**, and **success rate**, ensuring the system can quickly and accurately visualize vibration patterns, providing solutions. For data collection, the key parameters were sensor characteristics, such as **resolution**, **repeatability**, **response time**, **frequency response range**, and **error range**. These specifications were obtained by evaluating parameters for commercial sensors and are relevant for the identified customer requirements, such as capturing accurate and reliable vibration data.

- Resolution: The smallest detectable change in the measured variable by the sensor.
- Repeatability: The sensor's ability to provide the same output for repeated measurements under unchanged conditions, crucial for accurate vibration capture.
- Response Time: The time the sensor takes to respond to a change in the measured variable, impacting the speed of data capture.
- Frequency Response Range: The range of frequencies over which the sensor can accurately measure the variable, ensuring all relevant vibrations are detected.
- Error Range: The range within which the true value lies considering all potential sources of error, essential for accuracy.

After normalizing the scores, we found that the system's processing time and the sensor's frequency response range received the highest scores, followed by the mass and volume of the overall product, as well as the sensor's repeatability, response time, and success rate. These are highlighted in yellow and green in Illustration 2–1. This prioritization aligns well with the customer requirements and we will focus on these specifications during our project devel-

opment. For each customer requirement, we identified at least one engineering specification with a strong correlation (9 points), except for "Stability", "Easy Installation", "Less parts needed", and "Appealing Design", which had lower weighted importance or were inherently addressed by the overall product design.

Target values for these specifications were agreed upon with the company and benchmarked against commercial products. Specifications like mass, volume, processing time, and system success rate were directly provided by the company based on their machinery and needs. The project budget guided the target price, set at 4000 RMB. Sensor specifications were derived from averages of commercial sensors available on Amazon. We will try to meet the target values when deciding the types of sensors we will use in the project.

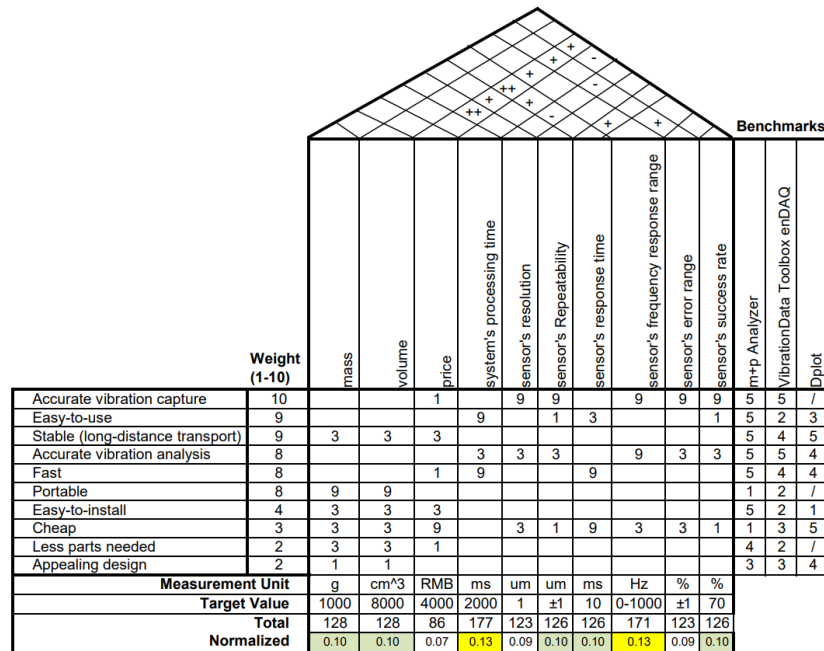


**Illustration 2-1 Quality Function Development chart for the project. Engineering specifications highlighted in yellow are the most important ones, followed by those highlighted in green.**

## Chapter 3 Concept Generation and Selection

### 3.1 Concept Morphological Analysis

The entire design is classified into four categories: data acquisition, data transfer, analysis tools, and user interface. The objective is to select one concept from each category that best suits our project. These four categories are closely interconnected: data acquisition involves selecting devices to capture raw vibration data during the riveting process; data transfer involves choosing a micro-controller to convert analog signals to digital ones for computer processing; analysis tools are used to evaluate and offer solutions on minimizing vibration; and the user interface displays the vibration patterns and analysis results. After brainstorming and researching, we identified three concepts for each category, as listed in Illustration 3–1. For data acquisition, we considered various sensors including accelerometers, laser sensors, and capacity sensors. For data transfer, we evaluated the Arduino board, NI DAQ, and Raspberry Pi. For analysis tools, we compared Ansys, SolidWorks, and theoretical calculations. Finally, for the user interface, we assessed three Python frameworks: PyQt, Kivy, and Tkinter.

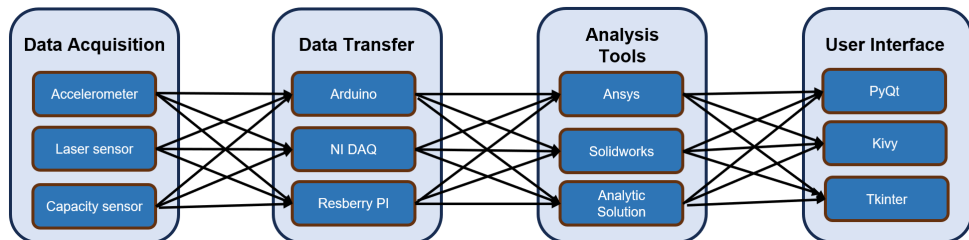


**Illustration 3–1 Morphological analysis chart. Each arrow represents a potential path that, when linked together, generates a concept that can be used to realize the whole design for our project.**

### 3.2 Concept Evaluation

#### 3.2.1 Sensor Selection

Sensor selection is crucial for this design, as it closely related to the most important customer requirement: accurate vibration capture. For each of the three sensor types, we

identified one commercial product available from Jing Dong: the **SG-MEMS-XYZ-V1 accelerometer**, the **Keyence IL-S030 laser sensor**, and the **enDAQ S3-D16 capacity sensor**. We compared the parameters of these three products based on the following criteria, ranked from most to least important: price, resolution, sampling rate, mass, repeatability, error range, volume, and frequency response range. These criteria were directly extracted from the engineering specifications in the QFD chart that were related to sensors; detailed explanations for their meanings can also be found in Section 1.3 of this report.

Illustration 3–2 includes the quantitative comparisons of these three sensors. Among these criteria, price and resolution were given the highest weight due to their importance in balancing performance and budget. Typically, a higher resolution sensor comes at a higher price, so our goal was to find the highest resolution sensor within our budget. The rest criteria were assigned similar weights, as in our opinion, they are equally important for evaluating sensor performance. In the end, the Keyence IL-S030 was selected because it offers high resolution at a reasonable price and does not require direct contact with the measured part. This is particularly advantageous for our project, since the measured part is small. The SG-MEMS-XYZ-V1 accelerometer, despite its low price and small size, requires direct placement on the measured part, making it unsuitable for our needs. The enDAQ S3-D16, while lightweight and highly accurate, exceeded our budget. Thus, the Keyence IL-S030 emerged as the optimal choice for our project.

Design Criterion	Weight factor	Unit	Accelerometer SG-MEMS-XYZ-V1			Laser Displacement sensor KEYENCE IL-S030			Capacity sensor enDAQ S3-D16		
			Value	Score	Rating	Value	Score	Rating	Value	Score	Rating
Price	0.2	RMB	950	10	2	2500	7	1.4	7000	1	0.2
Mass	0.11	g	50	9	0.99	60	8	0.88	16	10	1.1
Volume	0.1	mm^3	18900	10	1	36719	8	0.8	34061	8	0.8
Resolution	0.14	um	1.5	7	0.98	1	10	1.4	0.1	10	1.4
Repeatability	0.11	um	1	10	1.1	1	10	1.1	1	10	1.1
Sampling Rate/Period	0.13	ms	0.04	10	1.3	0.33	9	1.17	0.31	9	1.17
Frequency Response Range	0.1	kHz/mm	6	6	0.6	30	9	0.9	32	9	0.9
Error Range	0.11	%	2	4	0.44	0.1	9	0.99	0.1	9	0.99
<b>Total</b>					<b>8.41</b>			<b>8.64</b>			<b>7.66</b>

**Illustration 3–2 Concept evaluation matrix for sensor. The concept highlighted in green has the highest total score and will be selected. It is followed by concepts highlighted in yellow and red.**

### 3.2.2 Micro-controller Selection

Based on our group's experience, **NI DAQ**, **Arduino**, and **Raspberry Pi** were proposed as potential micro-controllers as they all have been used by some of us in previous courses. They were evaluated based on price, mass, volume, clock speed, number of I/O interface, and ease-of-use. In addition to price, mass, and volume, which were included in the engineering specifications, new evaluation criteria were added, as the rest specifications were not targeted for micro-controllers and relying on those three alone may not help us find the best concept. For these new criteria, clock speed determines the number of cycles a micro-controller can execute per second. A higher clock speed is desired, because it enables faster processing and better real-time data capture. The I/O interface represents the number of input and output ports the micro-controller has for interacting with other devices. Since our project requires at least one analog port to receive data from the sensor, higher weights were assigned to this criterion. Ease-of-use was rated on a scale of 1 to 5, based on factors such as development time and learning curve. Given that the user interface was the result to be shown to the sponsor, our group prioritized minimizing time spent troubleshooting code regarding data collection.

Illustration 3–3 shows the detailed comparisons where Arduino stood out due to its lowest price, smallest size and weight, and ease of coding, as all ECE students in the group had prior experience with it. Although Raspberry Pi has the highest clock speed, itself can function like a tiny computer, whereas our project only requires converting analog signals to digital ones. Thus, using Raspberry Pi would be overkill. NI DAQ was rejected as an option due to its high price and large volume.

Design Criterion	Weight factor	Unit	NI DAQ			Arduino			Resberry Pi		
			Value	Score	Rating	Value	Score	Rating	Value	Score	Rating
Price	0.28	RMB	3500	2	0.56	150	10	2.78	600	6	1.67
Mass	0.06	g	500	7	0.39	25	9	0.50	45	8	0.44
Volume	0.11	cm^3	2000	5	0.56	35	8	0.89	80	7	0.78
Clock speed	0.11	MHz	200	8	0.89	16	8	0.89	1500	9	1.00
I/O Interface	0.22	1-5	4	8	1.78	4	8	1.78	5	8	1.78
Ease-of-use	0.22	1-5	3	6	1.33	5	9	2.00	4	7	1.56
Total	1.00				5.50			8.83			7.22

**Illustration 3–3 Concept evaluation matrix for micro-controller. Arduino has the highest total score and will be selected. It is followed by concepts highlighted in yellow and red.**

### 3.2.3 Analysis Tool Selection

To understand the vibration patterns and propose solutions, we considered three methods: **Ansys**, **SolidWorks**, and **Theoretical Analysis**. Beyond the criteria mentioned in engineering specifications, we evaluated these tools also based on model geometry accuracy, material properties, ease of implementation, post-processing and visualization, frequency analysis, and automation.

- Model Geometry Accuracy: Minimizes discrepancies between the actual and modeled geometry.
- Material Properties: Saves time and ensures consistency with validated material data.
- Ease of Implementation: Measures how user-friendly the tool is for quick setup without extensive training.
- Post-Processing and Visualization: Helps interpret results, making it easier to identify key performance indicators and failure points.
- Frequency Analysis: Understands the natural frequencies and modes to avoid resonance and ensure structural integrity.
- Automation: Ensures consistent application of methods across multiple simulations, reducing human error.

For our project, model geometry accuracy and automation were given the highest weight, as our goal was to build an accurate model efficiently. As shown in Illustration 3–4, Ansys was selected for its strong performance in these areas. SolidWorks performed poorly in ease of implementation and frequency analysis. Theoretical analysis was inadequate in visualization and post-processing and required extensive theoretical knowledge, which was challenging for the two ME/MSE students in our group to master within one month.

### 3.2.4 User Interface Framework Selection

The user interface is another critical component of this project, as it is the primary point of interaction for users. Given our background as three ECE students and the simplicity of Python, we chose to use Python and proposed three popular frameworks: **Tkinter**, **PyQt**, and **Kivy**. Since the current engineering specifications include only "system's processing time" as a criterion for evaluating frameworks, to ensure a comprehensive evaluation, we proposed additional criteria:

Design Criterion	Weight factor	Unit	Theory (Analytical Solution)			SolidWorks			Ansys		
			Value	Score	Rating	Value	Score	Rating	Value	Score	Rating
Model Geometry Accuracy	0.2	mm	5	2	0.4	0.5	8	1.6	0.05	9	1.8
Material Properties	0.1	%	14	5	0.5	8	8	0.8	3	9	0.9
Ease of Implementation	0.1	#	5	8	0.8	4	6	0.6	3	4	0.4
Post-Processing & Visualization	0.15	#	2	4	0.6	4	7	1.05	5	9	1.35
Frequency Analysis	0.15	%	7	4	0.6	2	8	1.2	0.4	9	1.35
Automation	0.2	#	2	4	0.8	4	9	1.8	4	9	1.8
Cost	0.1	RMB	0	10	1	10500	6	0.6	105000	3	0.3
<b>Total</b>					<b>4.7</b>			<b>7.65</b>			<b>7.9</b>

**Illustration 3–4 Concept evaluation matrix for analysis tools. The concept highlighted in green has the highest total score and will be selected. It is followed by concepts highlighted in yellow and red.**

- Learning curve: The hours required for a Python programmer who has never used the framework before to learn it.
- Development speed: The time used to develop a standard user interface.
- Community support: The activeness of the community and the amounts of resources one can access.
- Response time (processing time): The start and response time for a standard program.
- Cross-platform support: The number of operating systems this framework supports, like Windows, Linux, macOS, Android, iOS.

The highest weight was assigned to response time, as capturing real-time vibration data depends not only on the sensor's sampling rate and the micro-controller's transfer speed, but also on the framework's data processing speed. Conversely, cross-platform support was assigned the lowest weight since all these frameworks support Windows, Linux, and macOS, which are sufficient for this project's scope. The remaining criteria focused on ease of learning and development speed, considering our limited time and beginner status to these frameworks. Illustration 3–5 shows the evaluation results, where PyQt received the highest score due to its fast response time, relative ease of learning, and strong community support. Although Tkinter and Kivy have a smaller learning curve, their processing times do not meet the project requirements.

Design Criterion	Weight factor	Unit	tkinter			PyQt			Kivy		
			Value	Score	Rating	Value	Score	Rating	Value	Score	Rating
Learning Curve	0.14	h	20	10	1.43	50	7	1.00	40	8	1.14
Development Speed	0.21	h	30	9	1.93	70	7	1.50	60	8	1.71
Community Support	0.18	1-5	4	8	1.43	5	10	1.79	3	6	1.07
Response time	0.36	ms	100	6	2.14	50	10	3.57	70	7	2.50
Cross-platform Support	0.11	#	3	6	0.64	4	8	0.86	5	10	1.07
Total	1.00				7.57			8.71			7.50

**Illustration 3–5 Concept evaluation matrix for user interface framework. PyQt has the highest total score and will be selected. It is followed by concepts highlighted in yellow and red.**

### 3.3 Concept Description

Based on the concept selection process, we have determined the components for our final product, as illustrated in Illustration 3–6. The design consists of a hardware set including a laser sensor, an amplifier, an Arduino board, and a 24V power supply. This hardware will be connected to a computer running the user interface, showing the vibration patterns. Additionally, we built CAD models and performed FEA simulations using Ansys. By simulating the entire radial riveting process, we identified parameters that minimize vibration (or the rivet's displacement) during riveting. The analysis and solutions obtained from these simulations will also be displayed in a dedicated section on the user interface.

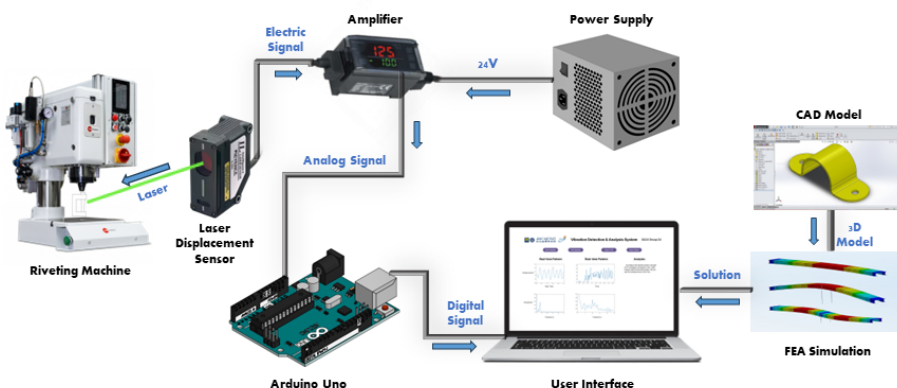


**Illustration 3–6 Concept diagram. The system was designed to receive and display vibration patterns from hardware, then show vibration patterns and solutions for minimizing vibration amplitude on the user interface.<sup>[1,22-28]</sup>**

The U-shaped part will be fixed on the riveting machine, with the sensor measuring the displacement of the point of interest during the riveting process. For data transfer among

the hardware components, the *Keyence* laser sensor captures raw displacement data as an electric signal, which is sent to its accompanying *Keyence* amplifier. The amplifier converts the electric signal to an analog signal, specifically voltage in our case. The Arduino board then maps the 0-5V voltage to a 20-45mm displacement, converting it to digital signals, and sending it to the computer. Finally, the user interface will display a real-time plot showing the displacement changes of the measured object.

## Chapter 4 Final Product Design

### 4.1 Final Design Overview

Using the selected concepts, we constructed the system with the components listed in Table 4–1. These components can be roughly classified into three main parts: sensor assembly, hardware set, and computer interface. The sensor, other than being placed together with other hardware components, is mounted on a tripod and secured with a sensor clip. The tripod ensures that the sensor remains stable and does not vibrate with the machine. Hardware set includes the rest supporting components for data collection such as a sensor amplifier, an Arduino board, and a power source. Lastly, a computer is needed to display the user interface and provides vibration pattern analysis results. These three components are connected with wires. We also included the U-shaped part as one of our designs for this project. Although it is not part of the vibration detection and analysis system itself, it is the object we are studying. The primary goal of this project is to address the vibration detection issues the company has faced with this U-shaped part in their collaboration with a multinational customer. Since this part caused significant issues, we prioritized its redesign and manufacturing to provide a basis for our study. Additionally, modeling this part and simulating the radial riveting process in Ansys is a crucial aspect of our product design as well, because the analysis of the vibration causes is based on these simulation results.

**Table 4–1 Major components for our vibration detection and analyzing system**

Component	Quantity	Usage
KEYENCE Laser Displacement Sensor IL-S030	1	Data Collection
KEYENCE Amplifier Unit IL-1000	1	Data Collection
Arduino Uno REV3	1	Signal Transformation
24V Power Supply	1	Power Source
Camera tripod	1	Holding Sensor
Sensor clip	1	Holding Sensor
Computer	1	UI Display

## 4.2 Detailed Designs

### 4.2.1 U-shaped Part

The design of the U-shaped part aims to address issues previously encountered in the company's collaboration with a multinational customer. This approach also allows Group 24 to efficiently manage resources, minimizing the number of rivets used for testing. Due to the joint between the rivet and the U-shaped part, it was not possible to reuse riveted items after one full riveting cycle. Additionally, manufacturing U-shaped part is time-consuming - it takes 2 hours to manufacture one U-shaped part using CNC equipment. Therefore, instead of using rivets, the decision was made to use bolts made of bare steel as they can simulate riveting process and not deform in a way that it is not possible to repeat the experiment with the same items after.

Quantitatively, bare steel, with an average yield stress of 2000 bars, is suitable for this purpose as the average input pressure during tests is 5 bars. This significant difference enables multiple experiments using one bolt instead of a rivet. The design, shown in Illustration 4-1, was chosen due to its low cost, the similarity to rivets, and the time savings in production. The sponsor company provided a package of bolts free of charge, as they had many available. All parts have been manufactured at the sponsor company's facility.

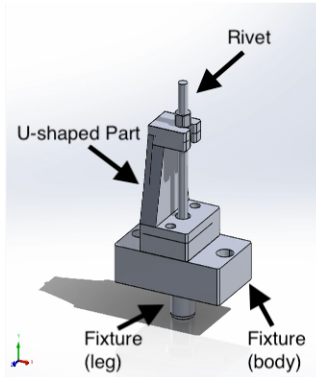


**Illustration 4-1 SolidWorks Model - U-Shaped Structure.** It illustrates the design of the tested sample and includes its subparts: the Fixture Leg, which connects the machine to the tested item; the Fixture Body, which holds the U-shaped part; the U-shaped part itself; and the Rivet.

During the design stage, two versions of the U-shaped part were considered, with varying widths for the middle section that connects the bottom and top cantilever beams. The detailed sketch is shown in Illustration 4-5(a). The decision to vary the width and analyze

its impact on vibrations was guided by the formulas for natural frequency  $f_1$  and deflection  $\delta$  of a cantilever beam, as given in Equation 4–1 and 4–2:

$$f_1 = \frac{1.875^2}{2\pi} \sqrt{\frac{EI}{\rho AL^4}} \quad (4-1)$$

$$\delta = \frac{FL^3}{3EI} \quad (4-2)$$

where in these equations,  $E$  represents the Young's modulus of the material,  $I$  is the second moment of area (moment of inertia),  $\rho$  is the density of the material,  $A$  is the cross-sectional area,  $L$  is the length of the beam, and  $F$  is a point load.

Given that changing the material was not feasible due to its cost-effectiveness and relevance to the actual scenario the company faced, modifying the cross-sectional area of the U-shaped part would be more costly than altering the width of the middle section, as any change in the cross-section would require a corresponding adjustment to the other beam to maintain symmetry, which would incur additional expenses. Therefore, adjusting the width of the middle section was deemed more practical and economical. This modification impacts the length  $L$ , as shown in Illustration 4–5(a), and subsequently affects the vibration characteristics. According to vibration theory, an increase in  $L$  leads to a lower natural frequency and a higher amplitude of vibration. The open top cantilever beam design allows for easy insertion and removal of bolts during experiments. Shorter bolts are used to simulate bending under a constant force applied to the right part of the top cantilever beam. This scenario mirrors the deformation of a rivet contacting the top surface of the cantilever beam, leading to the bending scheme detailed in the Appendix section of this document.

The fixture body and leg were designed in accordance with the machine parameters for fixtures, which are standardized based on the machine model, size, and applied input parameters. The material for the fixture was selected based on manufacturing and supply costs. Stainless steel, with an average yield strength of 4000 bars, was chosen to minimize stress-induced expansion and potential machine damage. A sketch of the entire testing apparatus, shown in Illustration 4–5(b), is provided with dimensions in millimeters.

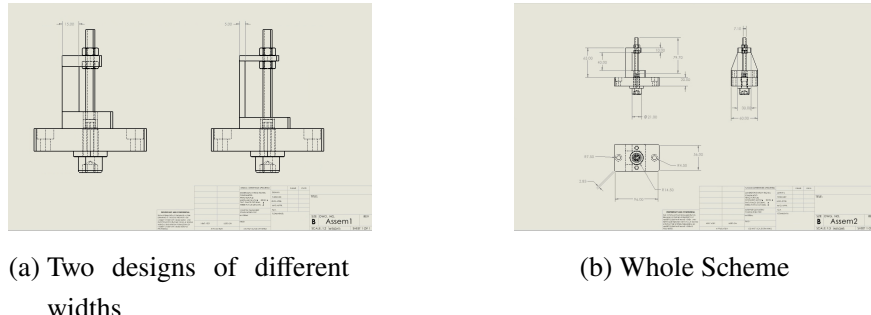


**Illustration 4–2 U-shaped part design details:** (a) Dimensions for 2 types of the U-shaped part with varying different width but identical other dimensions. (b) SolidWorks drawing that shows all required dimensions for manufacturing; pre-made bolts for joint are neglected in the picture.

#### 4.2.2 Data Collection Hardware Set

To achieve the project goals of measuring vibrations during riveting processes, the fundamental engineering principle employed is Light Detection and Ranging (LiDAR) technology for distance measurements. The sensor used in this project, the *Keyence IL-S030* laser displacement sensor, utilizes the triangulation method for distance measurement. This process involves emitting a laser beam from the sensor, which reflects off the target object. The reflected light is then detected by a CMOS sensor, and the position of the light spot on the CMOS changes with the distance to the target. This variation enables precise distance measurement through triangulation, calculated using the following formula:

$$d = \frac{L}{\tan(\theta)} \quad (4-3)$$

where  $d$  is the distance to the target,  $L$  is the baseline distance between the laser emitter and the detector, and  $\theta$  is the angle of incidence.

To analyze the vibration data, Fast Fourier Transform (FFT) is used to convert the time-domain signal into the frequency domain. This method allows for the identification of vibration frequencies and amplitudes, which is critical for understanding the characteristics of the vibrations. In this project, the FFT is applied to the measured distance data to determine the frequency components of the vibrations. It's computed using the formula:

$$X(f) = \sum_{n=0}^{N-1} x(n) \cdot e^{-j2\pi fn/N} \quad (4-4)$$

where  $X(f)$  is the frequency domain representation,  $x(n)$  is the time-domain signal,  $N$  is the number of samples, and  $f$  is the frequency.



**Illustration 4-3 Data Collection Overview:** Our final product primarily comprises three components: a laser sensor mounted on a tripod, an encapsulated hardware set containing supporting hardware like Arduino micro-controller, amplifier and power supply, and a computer for user interface display.

In Illustration 4–3, the laser is mounted on a bracket and aimed at the U-shaped part, which is fixed on the operating desk of the riveting machine. All hardware, including the sensor amplifier unit (Keyence IL-1000), the Arduino board, and the power supply, is encapsulated in a 3D-printed container to ensure neat wire organization. The hardware connects to the computer via the USB port linking the Arduino to the computer, on which the distance and corresponding FFT results are displayed. The project utilizes the *Keyence IL-S030* LiDAR sensor for distance measurement and the Arduino Uno R3 microcontroller for data acquisition and transmission. Although the *Keyence IL-S030* sensor supports a sampling rate of up to 3 kHz, we have configured it to 100 Hz in our project for two main reasons. First, during experiments, the observed vibration frequency was below 50 Hz. According to the Nyquist sampling theorem that states "an analog signal can be digitized without aliasing error if and only if the sampling rate is greater than or equal to twice the highest frequency component in a given signal.<sup>[29]</sup>", a 100 Hz sampling rate is sufficient to accurately capture these vibrations. Second, while a higher frequency could potentially capture a more accurate and smooth vibration pattern by obtaining more data points, it could also lead to data accumulation in the serial port, causing processing delays. Therefore, after testing, 100 Hz

proved to be the more appropriate choice.

#### 4.2.3 User Interface

Detailed design and function of the user interface can be found in Illustration 4–4. Developed using PyQt, the interface enables the collection of distance measurements and provides interactive functions for data visualization and analysis. The interface features four major sections: The Displacement Graph displays displacement measurements over a user-defined sampling period. The graph is automatically shown in this position on the UI after the sampling period ends. The FFT Result Graph shows the frequency domain representation of the vibration data, calculated based on the displacement data of the period. Since the vibration is small, to better illustrate the changes, the scale of the x-axis and y-axis for both these two plots will automatically adjust around the first 20 data points obtained, making sure the pattern is shown on the center of the graph. Additionally, the first three frequency peaks are highlighted as red points on this FFT plot, and their frequencies and corresponding amplitudes are summarized in the Text Box areas. Another area summarizes our findings, indicating potential factors that impact vibration amplitude.

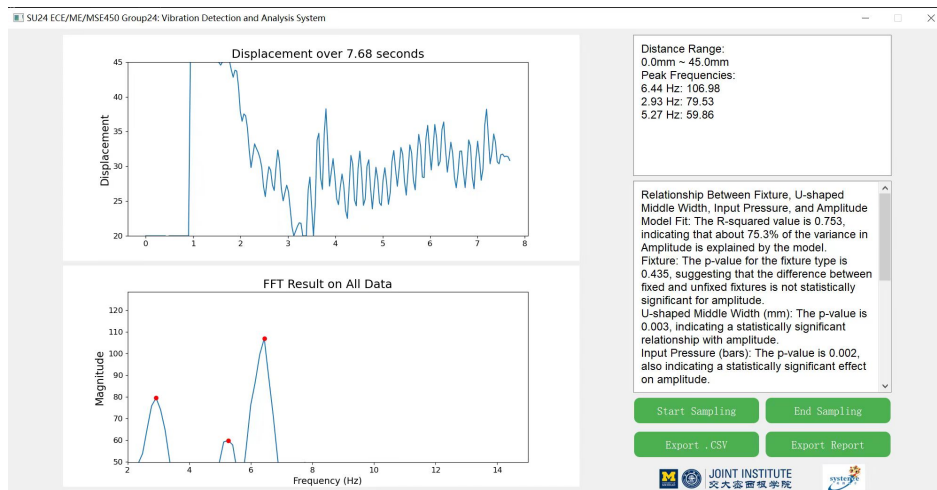


**Illustration 4–4 User Interface after sampling:** The left column contains two plots showing displacement changes during the riveting process and the corresponding FFT results. The right column features a text box displaying peak FFT frequencies during riveting and analysis results.

Below the text box are four buttons for starting and ending data collection, exporting raw vibration data in .csv format, and generating an analysis report.

There are four interactive buttons, highlighted in green in Illustration 4–4. The Start

**Sampling** button initiates the data collection process. Upon pressing, the system begins real-time sampling of distance data, and the text changes from "Click Start Sampling" to "Sampling" to inform the user that the process has started. This button supports multiple clicks, allowing users to restart the data collection process for multiple trials during a single program session. The **End Sampling** button stops the data collection process. When pressed, the UI displays the collected distance data and the corresponding FFT results for the entire sampling period, with the textbox providing an analysis of the obtained vibration data. Users can export the collected data and reports using the **Export .CSV** and **Export Report buttons**. The Export .CSV button allows users to export the collected distance data in CSV format, including all raw distance measurements taken during the sampling period. The Export Report button generates a report containing the distance and FFT result graphs, along with the analysis results, which can be used for further documentation or presentation purposes.

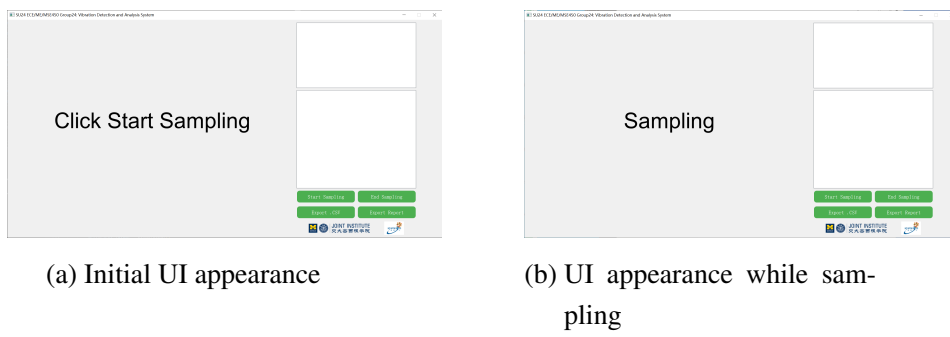


**Illustration 4-5 User Interface before and during sampling.** (a) shows the interface when the program is first loaded, providing guidance on how users can start the sampling process. (b) shows the interface during the sampling process, with hint words changing to indicate that the system is currently sampling.

#### 4.2.4 Modeling and Simulation

The purpose of modeling and simulation is to reproduce the radial riveting process on the U-shaped part using finite element analysis to identify parameters that can minimize vibration. The part was designed in SolidWorks based on the issue description the company had with their client, and simplicity in manufacturing and testing for this project. Thus, it can simulate the issue that happened in a real scenario and at the same time not be that consuming in terms of resources.

Subsequently, we imported the model into Ansys, which helps in determining the vibration modes of an object under specified conditions. 4 types of analysis have been used to simulate the riveting process and obtain the required data, which are **Static Structure**, **Modal Analysis**, **Harmonic Response** and **Transient Structural**. Static structural analysis involves evaluating the structural integrity of a component or assembly under static loading conditions. This type of analysis helps determine deformations, stresses, and strains in the structure when subjected to various forces, pressures, and moments. Ansys uses finite element methods to simulate how the structure responds to these loads (pressure induced by the riveting machine in our case), ensuring that the design can withstand the specified conditions without failure. Modal analysis is a technique used to determine the natural frequencies and mode shapes of a structure or component. This analysis identifies the specific frequencies at which the structure tends to naturally vibrate, which is crucial for understanding and preventing resonance-related issues. Those natural frequencies can be then transferred to the further analysis stages by superimposing those together. The point of connecting Static Structural and Modal Analysis is to prevent residual stress from the riveting process from altering the natural frequencies and mode shapes, potentially leading to issues if not properly accounted for.

The next two stages are separate from each other where one is used to find maximum and minimum values, and the second method is used in order to obtain the whole simulated data set during the test cycle. Harmonic response analysis is used to evaluate how a structure responds to sinusoidal (harmonic) loading over a range of frequencies. This analysis helps engineers understand the steady-state behavior of the structure when subjected to cyclic forces, such as vibrations from machinery or rotating equipment. By determining the amplitude of the response at various frequencies, harmonic response analysis identifies resonant frequencies and the associated deformation, stress, and strain levels. Transient structural analysis is a dynamic analysis method used to determine the response of structures to time-varying loads. Unlike static analysis, which considers only steady loads, transient analysis evaluates how structures behave under time-dependent forces, such as impacts, oscillations, or varying pressure loads. Once the time-domain data is obtained, it can serve as an input dataset for our FFT algorithm and provide frequency-domain analysis results.

The main point of conducting all those stages of analysis is to get deformation and fre-

quency values that have reasonably small differences compared to the data obtained from the actual riveting process. It gives a chance for more efficient optimization and potential benchmarking once the riveting process can be accurately simulated in Ansys.

## Chapter 5 Manufacture and Validation Results

### 5.1 Manufacturing Plan

#### 5.1.1 U-shaped Part

The manufacture process of the U-shaped part involves three main steps, each utilizing a different processing machine. First, **Electric-discharge Machining (EDM)** was used to create the main geometry of the U-shaped part. EDM is preferred for its ability to precisely machine complex geometries and intricate contours that are difficult to achieve with traditional methods. Additionally, EDM does not require direct mechanical contact, eliminating stresses and deformation on delicate or thin sections. It also works well with hard and brittle materials, providing high surface finish quality and maintaining tight tolerances essential for advanced engineering applications. After obtaining the main geometry, a **milling machine** was used to create the necessary holes in the part. Milling allows for accurate control over dimensions and tolerances, ensuring the finished product meets stringent specifications. Its ability to perform various operations such as cutting, slotting, and contouring on a single setup increases efficiency and reduces production time. Finally, a **grinder machine** was used to achieve a high surface finish quality. In terms of the sub-components of the U-shaped part, the fixture leg was pre-made by the company using butadiene rubber. During the entire manufacturing procedure, the fixture's dimensions were of the highest importance; if its accuracy was not met, the U-shaped part could not be properly held during experiments.

#### 5.1.2 Hardware Connection and Encapsulation

All hardware components were purchased or borrowed from the sponsor company, so our project did not involve a direct manufacturing process. However, given the numerous components and wires, we used SolidWorks to design a box that encapsulated all these components. Tapes were used to secure the wires, ensuring the connections would not break and the setup remained stable during transport. Measurements of each component's size and the placement of holes for wire access were incorporated into the SolidWorks model. The final product was created using 3D printing. This procedure resulted in a neatly encapsulated electrical component box, making it easier to transport.

Regarding the hardware connections, the laser sensor and sensor amplifier, both produced by Keyence, were connected through cables. The amplifier has 12 wires, as shown in Table 5–1, but in this project, we only used the analog input and output and voltage input and output wires. The two wires for voltage supply were connected to the 24V power supply. To link the analog signal to the Arduino board, we used the A1 port on the Arduino and read this port from the computer to obtain the digitized signal. The Arduino is connected to the computer via a USB interface. With this connection, the raw vibration data can be transferred smoothly as digital signals to the computer.

**Table 5–1 IL-1000 Amplifier Wire Diagram**

Color	Connect to
Brown	10-30 VDC
Blue	0V
Black	High decision output
White	Low decision output
Gray	Go decision output
Green	Warning output
Orange	Analog output (+)
Light Blue	Analog output (GND)
Pink	External input one (zero offset input)
Yellow	External input two (reset input)
Pink Purple	External input three (timing input)
Purple	Don't use

### 5.1.3 User Interface

The user interface was built using the PyQt framework in Python. It includes the general layout of the interface, vibration pattern plotting, and FFT data calculation. The complete code is included in the form of a GitHub repository link in the Appendix. Below are vital code descriptions that enable the user interface's major functions.

For the whole user interface, we used two classes: `SerialReader` that connects with the Arduino Board and `VibrationFFTApp` that visualizes all the contents on the interface. In addition to the `__init__` function in these two class objects, the `SerialReader` class has the following functions: init serial, read from serial, start and end receiving, and close

serial; these functions handle the reading port and sampling rate declarations.

The `VibrationFFTApp` class plays another important role in visualizing and arranging all contents that users see on the user interface. It includes functions such as init UI, start sampling, data plotting, export csv and export report, etc. In terms of specific designs, in PyQt, `QWidget` is the base class for all UI objects. Features such as buttons, labels, and vibration plots were held in these types on our UI. To better arrange the order of different widgets, `QVBoxLayout` and `QHBoxLayout` were used to arrange contents in a horizontal or vertical order. To include widgets in a layout, the function `addWidget` was used. On the user interface, we classified the main layout into two vertical layouts: the left one containing two vibration plots and the right one containing text areas, buttons, and logos.

Vibration data obtained through the port will be stored in a list. Based on the riveting time we have for the experiments, it would not exceed the memory even when the sampling rate is 100 Hz and there are many data points. The Fast Fourier Transformation (FFT) on the displacement data is realized through the `np.fft.fft` and `np.fft.freq` functions.

#### 5.1.4 Modeling and Simulation

The logical relationship between the four types of the analysis presented in the final design section is shown in Illustration 5–1. Each module is interconnected by lines of different colors. Blue lines indicate the four modules share common initial conditions, including engineering data, geometry, and model parameters that were established during the project's creation phase. Pink lines indicate the calculation results from the previous module are used to initialize the configuration of the subsequent module.

To begin, we imported the U-shaped model, including material properties and structure, into the **Static Structural** module. This module is used to analyze the response of structures under static loading conditions. To simulate the vibration process, we designated the bottom plane of the part as a fixed support and applied a vertical downward force along the center axis of the rivet at the top, as illustrated in Illustration 5–2(a). After performing the operation, we obtained the distribution diagram of total deformation, as shown in Illustration 5–2(b). This diagram illustrates the extent of deformation in each section of the U-shape when subjected to the fixed force. Additionally, the maximum and minimum principal stress and shear stress were also determined in this operation. With this Static Structural Analysis, we can further

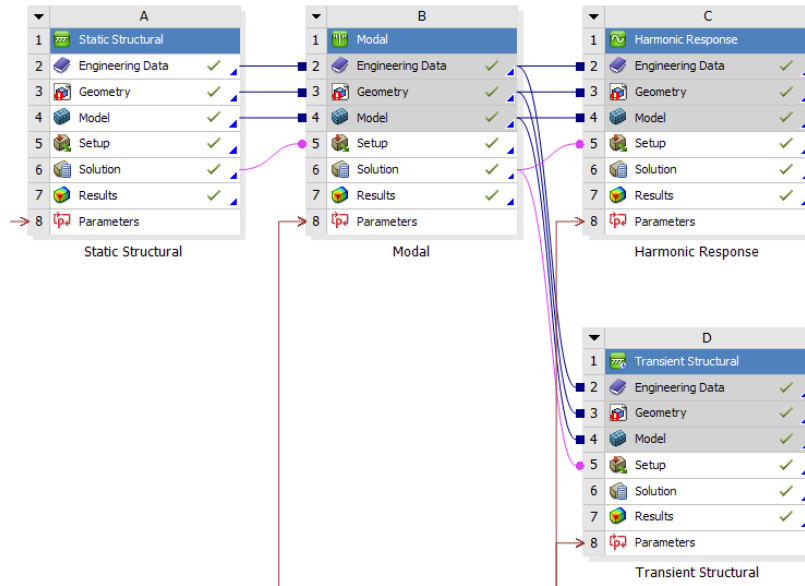


**Illustration 5–1 Ansys Workbench Overview.** Four modules are linked linearly: blue lines indicate shared initial conditions across all modules, while pink lines represent the transfer of calculation results from one module to initialize the next.

conduct comparative analysis by changing boundary conditions like the magnitude of the input force.

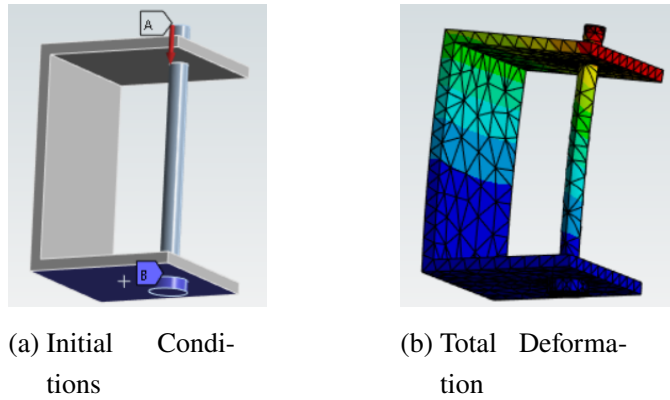


**Illustration 5–2 Modeled U-shaped part in Ansys:** (a) Initial condition: force A = 800N acts vertically on the top of the rivet, with plane B as the fixed support. (b) Distribution of total deformation: red indicates the maximum principal stress, and dark blue indicates the minimum principal stress.

Based on the data and the initial condition configurations we obtained from Static Structural Analysis, we used the **Modal** module to determine the natural frequencies and mode

shapes of the U-shaped part. The principle is to decompose the object into finite elements, calculate each element independently, and then superimpose the results to approximate the prediction of the vibration behavior. Mode and corresponding frequency is listed in Table 5–2. Additionally, Modal analysis provides the requested number of modes which later can be used for the superposition and harmonic analysis.

**Table 5–2 Modal Data Table**

Mode	Frequency [Hz]
1	774.36
2	969.87
3	3762.4
4	4411.0
5	5201.6
6	5985.2
7	6702.3
8	6776.1
9	7236.7
10	9571.8
11	12908
12	13472

After obtaining frequency values, it becomes possible to determine the steady-state response of structures under sinusoidal (harmonic) loads, which helps to understand the behavior of structures under dynamic loads. This analysis provides frequency response plots that illustrate the relationship between frequency and phase angle, as well as the relationship between frequency and amplitude, shown in Illustration 5–3. This procedure allows us to determine frequencies that result in the largest/smallest amplitude values.

Lastly, the **Transient Structural** module was also tested to ascertain the time-dependent response of the part when subjected to dynamic loading conditions. Based on the acquired steady-state response results and the initial conditions from the previous module, new vibration data closely resembling the real riveting process can be obtained through calculations. After being transformed through FFT, data simulated from this module can be compared with data obtained through our data collection system for validation. In the end, by varying factors such as force magnitude, material properties, and structural design, we can provide

suggestions on minimizing vibrations.

It is important to point out that with the current progress, we understand how to conduct a simplified simulation of our tested item in Ansys. However, there are several challenges that are present in this part of the project which are discussed in the more detailed way in the Analysis of Potential Problem section.

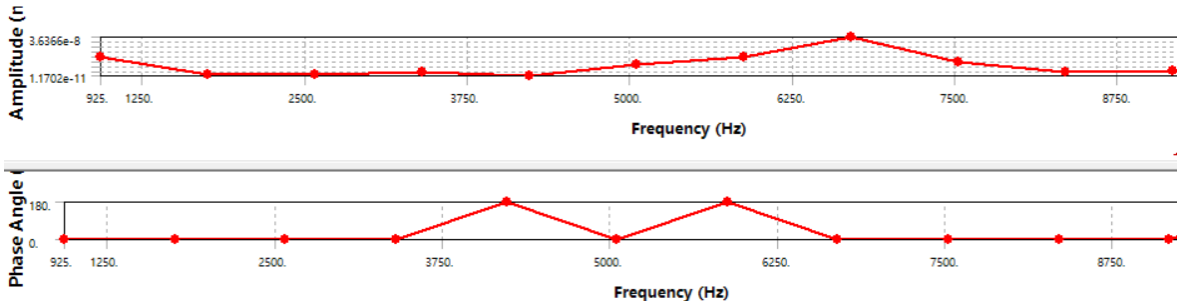


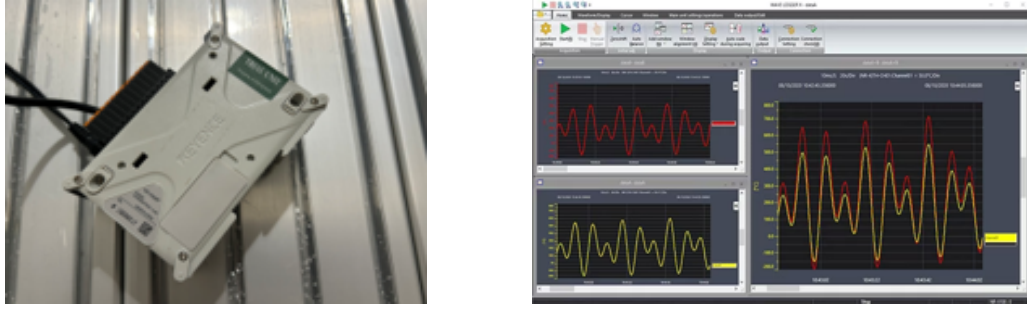
**Illustration 5–3 Simulated Frequency Response**

## 5.2 Validation

### 5.2.1 Validation Results

To validate whether our system can capture accurate vibration data, we used a commercial analysis device, the *Keyence* Trail Unit NR-500, and its corresponding software, shown in Illustration 5–4, as a reference. We believed that as a commercial product, it has the ability to accurately detect vibration problems in industrial production. Experiments were performed on the U-shaped part using both our system and the Keyence Trail Unit under the same conditions. Displacement data after each experiment could be downloaded from the Keyence Trail Unit Software shown in Illustration 5–4(b) as well as the "Export .CSV" function in our system. Data obtained from both measurements were plotted on the same axis, and the vertical distance between the two lines was measured to evaluate how closely our detected vibration pattern matched the one obtained from the commercial product. The percentage of closeness was calculated and used as our success rate. This approach ensured that we had a quantifiable measure of how well our system performed compared to an established commercial standard.

A 2-level full factorial design was utilized to provide experimental trials for our system



(a) Trial Unit NR-500

(b) Trial Unit Software Interface

**Illustration 5–4 Keyence Trial Unit.** (a) Outward appearance of the product, featuring analog and USB ports for connection with the laser sensor and computer. (b) User interface for Keyence’s trial unit, which allows users to start sampling, end sampling, adjust axis ranges, and export data.

validation and to investigate the relationship between three input factors that might influence vibration values during the riveting process, potentially leading to inaccuracies. Table 5–3 shows the summary for these two types of experiments. The riveting machine parameters included ground height setup for rod control and pressure values (2/5 bars). The U-shaped part was either fixed using bolts with the fixture body or simply positioned on the fixture’s top surface without any joints. Two types of U-shaped parts with different widths were tested. These input parameters were determined based on interviews conducted with the company regarding hypothetical parameters that could impact riveting, feasible levels of manufacturing, and investments required to change those. The output parameters, including peak frequency and amplitude values, were determined through FFT analysis of the collected data. This design of experiments (DOE) was selected to identify any statistically significant correlations between the input and output factors. The input parameters, represented by low and high values, are summarized in Table 5–3.

**Table 5–3 Input factors analyzed during the riveting process and values of those**

2-Level	Fixture	Width(mm)	Pressure(bars)
Low	unfixed	5	2
High	fixed	15	5

Since there were three parameters to be varied and to eliminate random errors during the experiments, each trial was conducted twice. According to the rule of controlled experi-

ments, where only one parameter is varied at a time, there are eight different combinations of parameters. After performing each combination twice, both our system and Keyence underwent 16 rounds of experiments. The experimental procedure involved setting up parameters on the riveting machine, installing the U-shaped part under the riveting rod, positioning the sensor for data collection, and running custom software for data collection and analysis. The custom software and riveting machine were operated simultaneously. Since both Keyence software and our system could only download the displacement data, we performed separate FFT analysis on each to determine the peak frequencies where vibrations occurred and plotted them on the same axis for comparison.

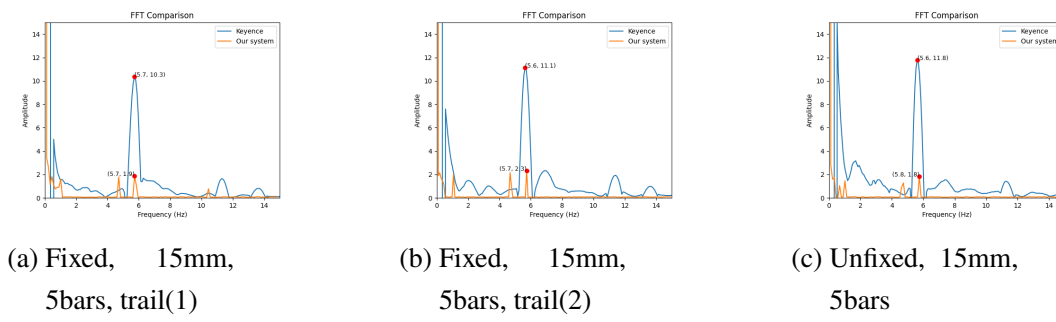


**Illustration 5–5 Validation results on the FFT plot for Keyence and our system. The orange line represents our system, and the blue line represents Keyence's. (a) and (b) show the FFT results obtained from the same setup, with our system showing similar results, which is reasonable. (c) shows the case when the fixture holding the rivet was unfixed.**

The validation results are summarized in Table 5–4. Results show that our system captures more accurate peak frequencies than amplitudes, with detailed explanations provided in Chapter 6. When the vibrations were significant, such as when the U-shaped middle width was 15mm and the input pressure was 5 bars, our system achieved a 75% accuracy rate in detecting the peak frequency. These two parameter setups resulted in larger vibrations because, according to the fundamental principles of dynamics, a larger force results in larger vibrations. Additionally, the larger width of the U-shaped part prevented bending during the riveting process, where bending typically presses the rivet to the part below it, reducing the vibration. Illustration 5–5 shows the three plots under this experimental setup, highlighting how well the peak frequency aligns with the benchmark, despite the significant difference in amplitude.

**Table 5–4 Validation results between our system and Keyence**

Experiment	Success Rate (freq)
All Trails	31.3%
Fixed	37.5%
Unfixed	25%
15mm Middle Width	37.5%
5mm Middle Width	25%
2bars Pressure	0%
5bars Pressure	62.5%
15mm Width and 5bars Pressure	75%
5mm Width and 5bars Pressure	50%

However, we found a notable discrepancy between the detection results of our system and Keyence's system when the vibration is small, in all detection of peak frequencies and amplitude. For frequency detection, only 31.3% of all 16 trials were within the 10% relative error range compared to Keyence's results, which is the threshold based on manufacturing rules for normal daily production. This low success rate could be due to the hardware limitations of the Arduino. In brief words, the actual vibrations on the rivet during the riveting process were very small, even below the minimum voltage difference that the Arduino could detect. Additionally, conducting only two trials for each parameter setup could result in insufficient data for stable experimental results.

### 5.2.2 Engineering Specification Analysis

Based on our concept selections and the final product design, we have successfully met most of the engineering specifications outlined in the QFD chart, except for the success rate of our system. Table 5–5 provides a summary comparison between the target values and the actual values obtained for our final product.

Mass and volume considerate primarily about the hardware set of the final product. Mass was validated using a scale and by measuring the dimensions of the container holding all the hardware components, total volume was determined. The price corresponds to the budget spent on building the final product and purchasing hardware components, excluding transportation costs. A detailed explanation for the minimal budget used is provided in Bill Ma-

**Table 5–5 Engineering Design Analysis Table**

Specifications	Target Value	Actual Value	Met requirement
mass	1000g	890g	Yes
volume	$8000\text{cm}^3$	$3073.6\text{cm}^3$	Yes
price	4000RMB	1004RMB	Yes
processing time	2000ms	15ms	Yes
sensor's resolution	$1\mu\text{m}$	$1\mu\text{m}$	Yes
sensor's repeatability	$1\mu\text{m}$	$1\mu\text{m}$	Yes
sensor's response time	10ms	0.33ms	Yes
sensor's frequency response range	1kHz	30kHz	Yes
sensor's error range	1%	0.1%	Yes
success rate	70%	31.3%	No

terial section in appendix. Processing time refers to the duration required for our system to refresh and update the real-time vibration plot. This was measured by calculating the time difference before and after each update in the software, with an average time of 15 ms. As probably could tell from the table, many engineering specifications are related to the sensor, as we believe selecting an accurate sensor for vibration detection is crucial for our project's success. These considerations were addressed during the sensor concept selection stage. Lastly, the system's success rate, which measures our ability to capture vibration patterns with no more than a 10% difference compared to the Keyence unit, was unfortunately only 31.3% due to hardware limitations. In Chapter 6, we included a detailed explanation of the approaches we took to try to overcome these challenges and discussions on how to improve this aspect.

### 5.3 Engineering Changes Notice

Since DR3, based on experimental results and problems encountered, we added several features and changes to the user interface to make it more user-friendly and accurate in terms of analysis. There are small changes in four main sections. Instead of hard coding the range of axes for the two plots, the system now automatically sets the x-axis and y-axis limits based on the first 20 sampling results, ensuring the graph is always centered for clearer interpretation. Second, peak frequencies in the FFT Result Graph are now marked with red points

for easier user identification and interpretation. The Text Box is now divided into two areas. Previously, we only displayed the dominant frequency and corresponding amplitude during the sampling process and how the displacement range was mapped from the voltage range. Now, an additional text area has been added to show the analysis results from our experiments. A scrollable bar was added to manage the space for the analysis text, preventing it from exceeding the display area. Lastly, the Start Sampling button now includes the function of repeating sampling when pressed again, initiating a new round of data collection. All buttons are programmed to be locked during program execution to prevent accidental pressing.

The sampling rate of the Arduino has also been adjusted to capture the high-frequency components during the vibration process. Previously, the main limitation preventing us from enhancing the sampling rate was the time-consuming process of updating real-time displacement plots and calculating FFT, which could result in data piling up at the port. We decided to forgo the real-time display of distance changes and FFT results. This trade-off allowed us to increase the UI animation refresh rate, boosting the sampling rate from 30Hz to 100Hz. We believe this decision is reasonable, as obtaining more data points and identifying larger peak frequency ranges is more important than displaying real-time plots.

The size of the encapsulation box also underwent parameter changes, as the previous design didn't leave enough room for larger components like the power source to fit in completely. Illustration in Appendix shows the ECN graph for the updated encapsulation design in SolidWorks. This change resulted in a box that perfectly holds all hardware components, making it easier to set up and transport. Changes in the encapsulation design can be found in the appendix section.

## Chapter 6 Findings and Discussion

### 6.1 Findings

By performing the 2-level full factorial design of experiments, we identified the parameters that significantly impact vibration amplitude. The data for analysis were derived from the Keyence trail unit, not our system, as validation results showed our system's measurements were not accurate. To ensure correct findings, we used the Keyence commercial product. Below are the statistical analysis results, which will form the basis for recommendations to the sponsor company on potential vibration elimination strategies.

Table 6–1 demonstrates the relationship between Fixture, U-shaped Middle Width, and Input Pressure versus vibration amplitude and peak frequency. A p-value threshold of 0.05 was selected; parameters with p-values smaller than 0.05 are considered significant. Based on the collected data, the p-value for the fixture suggests that the difference between fixed and unfixed fixtures is not statistically significant for amplitude. However, the p-values of the U-shaped Middle Width and Input Pressure indicate a statistically significant relationship with amplitude. Additionally, in the case of all the input (controlled) parameters, the p-values suggest no statistically significant effect on frequency.

The model fit tells us how well our chosen independent variables (Fixture, U-shaped Middle Width, and Input Pressure) can predict or explain the variation in our dependent variables (Amplitude and Frequency). For the current experiment analysis, the decision was made to use R-squared. The R-squared value for Amplitude is 0.753, indicating that about 75.3% of the variance in Amplitude is explained by the model. However, the R-squared value of the Frequency is 0.160, meaning only 16% of the variance in Frequency is explained by this model, which is quite low. A low R-squared value indicates that the model does not

**Table 6–1 Input Factors vs p-value results for amplitudes and frequencies**

Input Factor	p-value (Amplitude)	p-value (Frequency)
Fixture	0.435	0.574
U-shaped middle width (mm)	0.003	0.531
Input pressure (bars)	0.002	0.239

explain much of the variability in the dependent variable.

Based on the results, vibration amplitude is significantly affected by the width of the U-shaped part and input pressure. However, investigating the fixture is unnecessary when brainstorming potential solutions for vibration reduction, as it does not impact vibration amplitude. Additionally, the vibration frequency is not influenced by any of the factors. These conclusions are drawn based on the p-values, which are commonly used for testing parameter significance.

## 6.2 Discussion

### 6.2.1 Hardware Limitation

Since we did not know the vibration amplitude of the machine in advance, before the concept selection stage, we chose the Arduino microcontroller. However, during the experiments and validation stage, we found that Arduino's Analog to Digital Converter (ADC) was not accurate enough. Our research revealed that the ATmega8 microcontroller used by Arduino has six ADCs, each with a 10-bit resolution, meaning they can read 1024 states ( $2^{10} = 1024$ ). The voltage range on each analog input pin of the Arduino is from 0V to 5V, so the smallest detectable voltage change is 4.8 millivolts ( $5/1024 = 4.8mV$ ). Considering a distance range of 20mm to 45mm, the voltage is mapped to distance, resulting in a resolution of 0.0244mm. However, by using Keyence's equipment, we found that the change in distance is often less than 0.1mm, with changes between measurements even less than 0.02mm, indicating that Arduino is not accurate enough for distance measurements.

To address this issue, we designed an amplifying circuit based on the AD620, capable of amplifying the voltage by a factor of five, as shown in Illustration 6–1(a). To ensure the circuit can achieve a gain of 5, we used the equation 6–1 to calculate the external resistor that should be used:

$$R_G = \frac{49.4k\Omega}{G - 1} \quad (6-1)$$

where  $G$  is the desired circuit gain, which is 5 in our case. Additionally, a 12V power source was used to ensure the circuit could amplify the input voltage by 5 times. Illustration 6–1(b) shows the validation process of our amplifying circuit. The input waveform generator is set to 1V DC, and the digital multimeter displays an output voltage of 5.09V, indicating that our

amplifier circuit works.

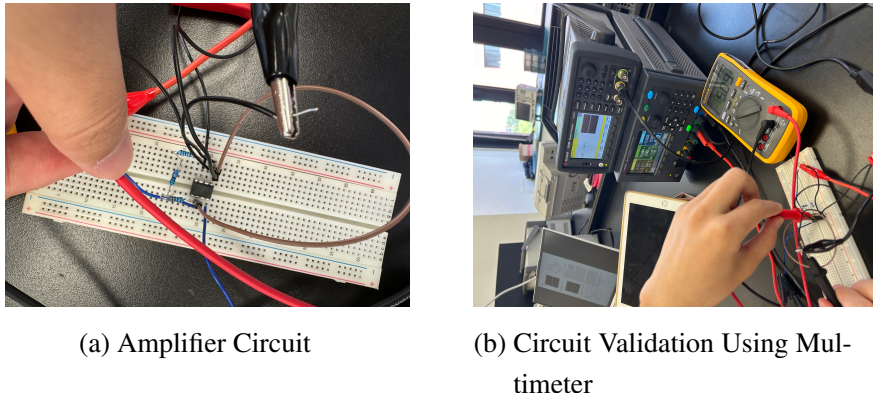


**Illustration 6–1 Amplifier Circuit based on the AD620 capable of amplifying the voltage by a factor of 5.**

Since Arduino can only receive voltages from 0-5V, and the smallest range of the sensor amplifier also outputs 0-5V, amplifying by 5 times would result in an output of 0-25V, which exceeds the Arduino's input range and could damage the hardware. Therefore, we carefully adjusted the sensor's position to the target object, ensuring the sensor's measurement range was limited to 40mm-45mm so that the sensor amplifier's output would be within 0-1V. After amplification, this still fell within the range of 0-5V. This output was then passed through the amplifier circuit and connected to the Arduino. However, this attempt ultimately failed. As illustrated in Fig. 6–2, the riveting process did not introduce any frequency peak. The noise introduced by the amplifier circuit was too large, drowning out the vibration signal. Hence, we abandoned the amplifier circuit.

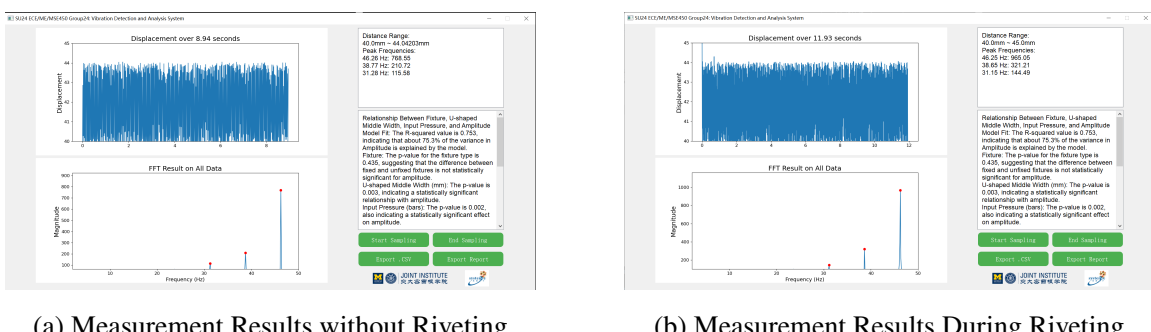


**Illustration 6–2 Measurement result comparison with amplifier circuit**

In practical experiments, despite the less-than-perfect distance measurement accuracy,

Arduino can still accurately capture the vibration frequency during the machine's riveting process. This might be because the imprecise data from Arduino still reflects the vibration pattern of the machine. For future improvements, since the Arduino code is straightforward, primarily sampling the voltage output from the amplifier connected to the laser sensor and converting it to distance before sending it to the computer, it will be easy to transition from Arduino to more precise equipment.

### 6.2.2 Ansys Simulation

We planned to use Ansys simulation to find parameters that would impact vibration amplitude by simulating the radial riveting our machine performs. However, Ansys proved to be more challenging to learn than anticipated. Although we ultimately obtained results by conducting actual experiments, we discuss below the challenges we faced in this task for future reference.

We failed to simulate the radial riveting pattern in Ansys. While simulating the one-dimensional path of the riveting die was feasible, radial riveting involves a two-dimensional trajectory that is more complex to simulate, which is also shown in Illustration 1–1(b) in Introduction chapter. One issue we encountered was not knowing the formula that describes the radial riveting path of the FMW Riveting machine used for this capstone project. We found one document describing the general path of a radial riveting die, but it was not product-specific. Another issue was the difficulty in finding the set of commands to set up and configure the required path using the x,y system of equations. The connection between the riveting die and the rivet is a half-joint, so they should not move as a single system; one should follow the radial riveting path while the other remains fixed. Imposed pressure and friction should then simulate the riveting process on the rivet.

Another challenge was the need to input the acceleration value with which the rivet deforms under pressure, which must be experimentally determined since it varies based on the required pressure and the initial and final heights of the rivet. It was unclear how to determine this pressure since, if it must be experimentally measured, it negates the point of simulating the process. Alternatively, it was unclear how to determine it using other methods.

Lastly, the previous two factors were identified as requirements without which the experiment could not be simulated. However, other important parameters might have been

overlooked or filled in with incorrect values. One such parameter is the number of modes required. Ansys allows for the input of any number of modes, which are then superimposed for further analysis. If the number of modes requested is insufficient to simulate the complicated geometry of U-shaped parts and rivets, it could lead to inaccuracies. This is just one example from a list of many similar parameters, each of which could introduce additional inaccuracies in the simulations.

### 6.3 Future works

Further investigating the relationship between input and output parameters presents a valuable opportunity for advancing this project. Our primary focus was to develop a system capable of efficiently collecting vibration data during the riveting process. While we identified statistically significant factors influencing vibrations, the next phase involves predicting output values based on input parameters.

To achieve this, we recommend starting with linear regression to quantify the relationships between input factors and output responses. Given the involvement of multiple factors, multiple regression analysis can be employed to develop a comprehensive equation that describes these relationships. For more complex predictive modeling, machine learning techniques such as decision trees, random forests, or neural networks can be considered. Cross-validation techniques will be essential to assess the performance and reliability of these predictive models.

Due to time constraints, our data collection and analysis were limited to one week, as the main goal of this project extended beyond this scope. However, with additional time and access to a riveting machine provided by the sponsor company, extensive data collection could be undertaken. This would shift the project focus towards data analysis rather than system development. Another promising direction for future projects is the simulation of the riveting process using software like Ansys. Successful simulation can significantly enhance the company's approach to item analysis. While our project involved multiple engineering disciplines, future studies could concentrate on specific aspects. Students can independently learn the basics of Ansys and vibration analysis, but guidance from an experienced mentor would be invaluable. Finding such expertise early on, possibly with university assistance, would greatly benefit the project.

This simulation approach offers the advantage of reducing the need for physical riveting machines. Students can perform simulations and then test the results at the company's facility, minimizing the company's investment. Additionally, simulations allow testing of a broader range of input factors, free from the constraints of manufacturing time, logistics, and costs.

## Chapter 7 Conclusion

Based on the experience of our sponsor company, Shanghai Systence, vibrations occurring during the riveting process are a major cause of inaccuracies in post-riveting results. The company provided an example involving a recent issue with a multinational customer where assembly parts varied significantly in dimensions despite the machine functioning properly. The riveted item in question consists of a U-shaped part and a rivet. Through interviews and brainstorming sessions with the sponsor company, we identified uncontrolled vibrations during riveting as the most likely cause. Thus, the problem we addressed for this capstone project was the study of vibrations occurring during radial riveting on the U-shaped part.

To draw quantitative conclusions about the impact of vibrations during joint formation, we needed data that could statistically show any correlations leading to inaccurate riveting. Additionally, the sponsor company had previously relied on experience and trial methods without tracking the impact of new design decisions on vibration reduction. Consequently, we decided to create a data-gathering system comprising both hardware and software components to evaluate progress in vibration reduction for the tested part. Our literature review on possible solutions indicated the need for an optimized U-shaped part, a data collection sensor, data processing hardware, and a software application capable of visualizing and analyzing the collected data points.

The tested item was optimized through discussions with company representatives, considering our project's budget and time constraints. We used the comparison matrix method to evaluate the final design parameters, which included a non-contact sensor, an Arduino microcontroller, a custom-developed user interface, and an Ansys simulation model to potentially test and optimize input parameters faster using a digital twin.

Our system can capture vibration displacement and identify peak frequencies and corresponding amplitudes in FFT results on the user interface we created. Additional features include buttons for users to customize the sampling period, and download CSV data and reports. Through experiments, we found that the pressure applied during the riveting process and the width of the U-shaped part significantly affect vibration amplitude, while the fixture's fixation has little impact on amplitude or frequency. However, due to hardware limitations,

our system achieves a success rate of 75% in experimental trials with large vibrations, while small vibrations result in notable differences from the reference benchmark, with a success rate of 31.3%. We attempted to increase the sampling rate by optimizing UI functions and eliminating real-time FFT visualization. Additionally, we built an amplifying circuit to enhance the voltage difference from the sensor amplifier, aiming to address hardware resolution limitations. However, this introduced noise that overshadowed the vibration signal. Nevertheless, this isn't hard to solve. Replacing Arduino with a higher-precision microcontroller would likely resolve this issue, though time constraints prevented us from making this switch during the project.

Additionally, although we did not create an accurate Ansys model to predict the behavior of the tested item during riveting, we gained valuable insights into the procedure for building such a simulation, including the necessary parameters for a realistic model. We also provided reasons for the company to continue this work post-project.

Using the design of experiments approach, our team quantitatively demonstrated the statistical relationships between several input and output parameters, achieving the initial goal of tracking design modifications from a vibrations perspective. This project represents the first step in identifying and controlling factors within the riveting process for more precise future adjustments.

## Acknowledgements

The team would like to extend our heartfelt gratitude to the following individuals and organizations for their invaluable support and contributions to the capstone project "Analysis of Vibration-Induced Measurement Inaccuracies in Riveting Processes."

We would like to express our appreciation to our section instructor, Prof. Peisen Huang, for meeting with us every week and offering helpful suggestions, drawing on his extensive research experience in the field of vibration. His patience and dedication in helping us acquire vital knowledge and skills have been truly inspirational. Our sincere thanks also go to the course instructors: Prof. Jigang Wu, Chengbin Ma, and Chong Han, for their invaluable suggestions during our Design Review presentations and reports writing. Their attentive listening and helpful feedback have been crucial in shaping our final thesis report.

We are grateful to our sponsor company, Shanghai Systence, for their tremendous support throughout the project. Special thanks to Mr. Yinsheng Su, Mr. Wen Liu, Mr. Aiguo Liu, and Mr. Yongzheng Yue for their mentorship, which has been crucial in helping us develop both personally and professionally. Their warm welcome during our visits and clear explanations about the machine and riveting process, which were new to most of us, have been invaluable. Collaborating with such a dedicated and talented team has been an inspiring and motivating experience and we sincerely appreciate the trust placed in us and the opportunities provided to contribute to this important project. We would also like to extend our appreciation to Mr. Jiale Huo from Keyence China for his great help in lending us the sensor and amplifier and guiding us in using the software.

Lastly, we would like to thank all our family members and friends. We could not have achieved this accomplishment without their unwavering support. After graduation, three of our group members will continue their studies in graduate school, while two will step into the professional world. We believe that the knowledge and experiences gained through this project, as well as the lectures and experiences of the past four years, will make a significant difference in our future lives. No matter where we are or what we are doing, we will always strive for higher achievements.

## References

- [1] FMW Friedrich Riveting Machine[EB/OL]. FMW Friedrich. [2024-06-11]. <https://www.fmw-friedrich.de/en/products/riveting-machines-and-riveting-units.html>.
- [2] Radial Riveting Patten[EB/OL]. BelTec. [2024-07-14]. <https://baltec.com/en/technologies/radial-riveting>.
- [3] Vibration & Temperature Sensor[EB/OL]. TURCK. [2024-06-18]. <https://www.turck.de/en/product/100016543>.
- [4] FLUKE. Fluke 820-2 LED Stroboscope[J/OL]. www.fluke.com, 2024. <https://www.fluke.com/en-us/product/mechanical-maintenance/vibration-analysis/fluke-820-2>.
- [5] EnDAQ. S3 Vibration Sensor[J/OL]. www.enDAQ.com, 2024. <https://endaq.com/collections/endaq-shock-recorders-vibration-data-logger-sensors/products/s3-vibration-sensor-s3-d16#>.
- [6] GARCIA Y R, CORRES J M, GOICOECHEA J. Vibration detection using optical fiber sensors [J]. Journal of Sensors, 2010, 2010(1): 936487.
- [7] LIU X, JIN B, BAI Q, et al. Distributed fiber-optic sensors for vibration detection[J]. Sensors, 2016, 16(8): 1164.
- [8] WENG Y, QIAO X, GUO T, et al. A robust and compact fiber Bragg grating vibration sensor for seismic measurement[J]. IEEE sensors journal, 2011, 12(4): 800-804.
- [9] SHUKLA A, MAHMUD M, WANG W. A smart sensor-based monitoring system for vibration measurement and bearing fault detection[J]. Measurement Science and Technology, 2020, 31(10): 105104.
- [10] GUO J, WU X, LIU J, et al. Non-contact vibration sensor using deep learning and image processing [J]. Measurement, 2021, 183: 109823.
- [11] KRODKIEWSKI J. Mechanical vibration[J]. The University of Melbourne Department of Mechanical and Manufacturing Engineering, 2008: 9, 28-34.
- [12] MOHD GHAZALI M H, RAHIMAN W. Vibration analysis for machine monitoring and diagnosis: A systematic review[J]. Shock and Vibration, 2021, 2021(1): 9469318.
- [13] YAN R, GAO R X. Hilbert–Huang transform-based vibration signal analysis for machine health monitoring[J]. IEEE Transactions on Instrumentation and measurement, 2006, 55(6): 2320-2329.
- [14] STASZEWSKI W. Wavelet based compression and feature selection for vibration analysis[J]. Journal of sound and vibration, 1998, 211(5): 735-760.
- [15] SARUHAN H, SARIDEMIR S, QICEK A, et al. Vibration analysis of rolling element bearings defects[J]. Journal of applied research and technology, 2014, 12(3): 384-395.
- [16] AMIHAI I, GITZEL R, KOTRIWALA A M, et al. An industrial case study using vibration data and machine learning to predict asset health[C]//2018 IEEE 20th Conference on Business Informatics (CBI): vol. 1. 2018: 178-185.
- [17] ZHAO Y, GUO Z H, YAN J M. Vibration signal analysis and fault diagnosis of bogies of the high-speed train based on deep neural networks[J]. Journal of vibroengineering, 2017, 19(4): 2456-2474.
- [18] PRUDHOM A, ANTONINO-DAVIU J, RAZIK H, et al. Time-frequency vibration analysis for the detection of motor damages caused by bearing currents[J]. Mechanical Systems and Signal Processing, 2017, 84: 747-762.
- [19] JUNG D, ZHANG Z, WINSLETT M. Vibration analysis for IoT enabled predictive maintenance

- [C]//2017 ieee 33rd international conference on data engineering (icde). 2017: 1271-1282.
- [20] TRENDAFILOVA I, CARTMELL M P, OSTACHOWICZ W. Vibration-based damage detection in an aircraft wing scaled model using principal component analysis and pattern recognition[J]. Journal of Sound and Vibration, 2008, 313(3-5): 560-566.
- [21] GRASSO M, CHATTERTON S, PENNACCHI P, et al. A data-driven method to enhance vibration signal decomposition for rolling bearing fault analysis[J]. Mechanical Systems and Signal Processing, 2016, 81: 126-147.
- [22] CMOS Multi-Function Analog Laser Sensor[EB/OL]. Keyence. [2024-07-15]. <https://www.keyence.com/products/sensor/positioning/il/>.
- [23] Keyence FW-V20P Positioning Sensor, Amplifier Unit PNP[EB/OL]. b2esurplus. [2024-07-15]. <https://www.b2esurplus.com/keyence-fw-v20p-positioning-sensor-amplifier-unit-pnp/>.
- [24] Power Supply Vector Figure[EB/OL]. VectorStock. [2024-07-15]. <https://www.vectorstock.com/royalty-free-vector/power-supply-unit-icon-in-monochrome-style-vector-13229273>.
- [25] Arduino Uno Vector Figure[EB/OL]. CRABCAD Community. [2024-07-15]. <https://grabcad.com/library/arduino-uno-28>.
- [26] iStock computer vector figure[EB/OL]. Getty Images. [2024-07-15]. <https://www.istockphoto.com/vectors/computer>.
- [27] SolidWorks Tutorial: How to Create U Bracket in Sheet Metal[EB/OL]. SolidWorks. [2024-07-04]. <https://www.youtube.com/watch?v=LMtHPEvPt3w>.
- [28] Designing Vibration Damping with Ansys Mechanical[EB/OL]. Ansys. [2024-07-04]. <https://www.cadfem.net/en/cadfem-informs/media-center/cadfem-journal/designing-vibration-damping-with-ansys-mechanical.html>.
- [29] CONSTANT N, CAY G, RAVICHANDRAN V, et al. Chapter 13 - Data analytics for Wearable IoT-based Telemedicine[G/OL]//Wearable Sensors (Second Edition). 2021: 357-378. <https://www.sciencedirect.com/science/article/pii/B9780128192467000139>. DOI: <https://doi.org/10.1016/B978-0-12-819246-7.00013-9>.

## Author Bios Appendix 1

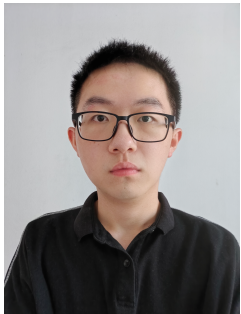


**Mansur Ayazbayev** - senior student at UMSJTUJI studying Mechanical Engineering. Passionate about connecting engineering knowledge with business best practices. Has a strong belief that it is important to know how to create a product and identify a group of people for whom this product could be useful and helpful. Did several internships in both engineering and business development roles at the projects including wind farm planning and construction, venture capital analysis, business development for a green tech startup, and e-commerce analytics. After graduation has a plan to start a career journey in a technological company based in Shanghai because of the love of Chinese food, the incredible pace of the economic development of this region, and desire to learn from the best. In free time hobbies include training, running, playing the guitar, singing, exploring bars in Shanghai, and going to KTV with friends. Likes working on projects that can have an actual impact and understands how actions lead to the development of the product, department, or the whole company. Not sure of the exact industry would like to spend the next 10 years in but trials and making a difference in real projects should be helpful to define what would be the best personally and for society. Again, learning and understanding the way Shanghai and China in general made this incredible economic jump in such a short time period is another goal that could also help shape Kazakhstan's economic path in the future.



**Jingtian Zhu** is a senior student majoring in Electronic and Computer Engineering. He has planned to work in financial area after graduation. When entering the college, he was ambitious about his following study life. But it struck him when the epidemic, physical and mental distort came together. He failed to follow up the majority. Thanks to the help and guidance from many people, he struggled to the end of the undergraduate term. He had made some academic research with the guidance of Prof. Qiao Heng in convex optimization algorithm and successfully reproduced

some newly designed methods. In this project, he will make market research to offer suggestions on specific problem solving and help develop the analysis software and UI interface. It is supposed that he will have a deep experience in entire process of engineering problem solving and apply it in the future career.



**Yiming Wang** is a senior student majoring in Material Science and Engineering. He has received the Freshman Merit Scholarship and Academic Progress Scholarship. During the first two years of his undergraduate study, he faced difficulties in his academics, partly due to personal reasons and the impact of the epidemic. Nevertheless, with the guidance of others and his own self-reflection, Wang managed to overcome these challenges and invested more effort into his academic pursuits. He had engaged in research projects involving Fourier spectrum analysis of polymers and Differential Scanning Calorimetry of metals, allowing him to accumulate valuable research experience. Through his participation in these projects, he has gained in-depth knowledge and practical skills in conducting research within the field. Upon graduation, he decides to pursue a master's degree in materials science. And in this project, he plans to initially research on the study of vibration theory, broadening his understanding of the subject matter. Subsequently, he will utilize his expertise to assist his teammates in sensor selection and modeling.



**Heng Zhao** is a senior student majoring in Electronic and Computer Engineering. He has received Fuda, Huatai Securities Research Scholarship. He has been admitted to the JI Computer Science and Technology master's program under the guidance of Professor Zhu Yifei. He has accumulated extensive research experience in various cutting-edge technological domains. From February to May 2022, he worked under Professor Zhang Quanshi on a project titled "Batch Normalization Is Blind to the First and Second Derivatives of the Loss." Following this, from May to October 2022, he collaborated with Professor Jin Haiming on ego-motion estimation for mobile platforms. His research journey continued from October

2022 to March 2023, where he worked with Professor Tang Aimin on joint communications and indoor localization via UWB. Since April 2023, he has been conducting research under Professor Zhu Yifei on a project titled "The Space above the Sky: Uniting Global-Scale Ground Station as a Service for Efficient Orbital Data Processing," with his first-author paper currently under review.



**Yujia Gao** is a senior student majoring in Electronic and Computer Engineering. She has been participating in the Graduate Degree Program, a collaboration between Shanghai Jiao Tong University-University of Michigan Joint Institute (SJTU-UM JI) and the University of Michigan. Through this program, she discovered her passion for Data Science and decided to shift her academic focus in that direction. Throughout her four years at JI, Yujia has concentrated on Electronic Engineering, engaging deeply in both coursework and research. One notable project she contributed to was under the guidance of Professor Yuljae Cho, where she worked on developing a piezoelectric sensor designed to measure human body pulses.

This research experience fueled her interest in applying engineering principles to practical, real-world problems. After graduation, she plans to continue her master's degree, and explore opportunities in Data Analysis and Business Analysis, as she is enthusiastic in working with numbers and communicating with people. As she prepares for this next chapter, Yujia is committed to leveraging her education and experiences to make meaningful contributions to this project.

## Bill of Materials Appendix 2

The major costs for this project are related to hardware purchases and transportation. Table 2–1 details the allocation and expenditure of our budget. Notably, the Keyence laser sensor and Keyence sensor amplifier are marked with a \*, meaning they didn't spend the actual budget, as during discussions with our sponsor company, we were informed that Keyence, one of their suppliers, would lend us these products. Nevertheless, we still decide to included them in the budget table to demonstrate that even with all costs accounted for, our total budget remained within acceptable limits, as we avoided purchasing high-value items to achieve our project goals.

**Table 2–1 Bill of Materials**

Quantity	Part Description	Purchased From	Price (each)
1	*KEYENCE Laser Displacement Sensor IL-S030	Keyence	¥2500
1	*KEYENCE Amplifier Unit IL-1000	Keyence	¥1500
1	Arduino Uno REV3	JingDong	¥169
1	Camera Tripod for Sensor Fixation	JingDong	¥35
2	3D printing	SJTU	¥26
10	Alligator Clip Wire	JingDong	¥1
20	Dopont Thread	JingDong	¥0.3
2	Transportation	Taxi	¥366
<b>Total</b>			¥5004
<b>Total (excluding *)</b>			¥1004

## ECN and Relevant Figures and Codes Appendix 3

### 3.1 Engineering Change Notice

Illustration 3–1 shows the differences in designing the encapsulation box in SolidWorks. The major change involved providing more space for the power supply. The bottom part of the power supply has numerous wire connections, necessitating a larger opening to accommodate it properly. From the figure, you can observe that an additional rectangular hole was designed above the original rectangular hole. This adjustment ensures that the power supply fits securely and the connections are easily accessible.

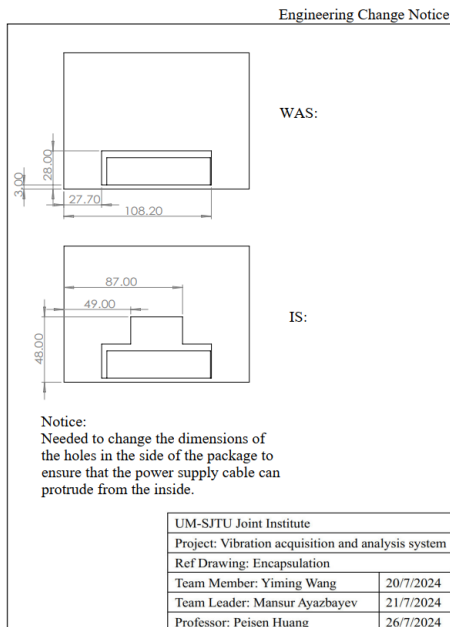
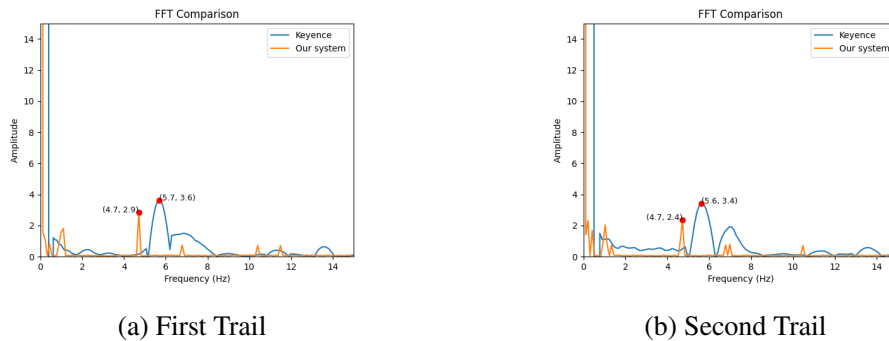


Illustration 3–1 ECN for encapsulation box

### 3.2 Validation Plots for Developed System

Below are the validation plots of our system compared to the reference Keyence software on the Fast Fourier Transformed (FFT) vibration pattern. Each setup in the experimental design was conducted twice and they were plotted side by side in the below Illustration for better comparisons. Three variables were considered in the experiments: fixation (whether

the U-shaped part is fixed or not during the riveting process), the middle width of the U-shaped part (15mm or 5mm), and the applied pressure on the rivets (2 bars or 5 bars). In all figures, the orange line represents the results obtained from our system, while the blue pattern represents Keyence's reference pattern. Peak frequencies are marked using red dots.



**Illustration 3–2 Fixed U-shaped part with middle width 15mm and 2 bars pressure.**

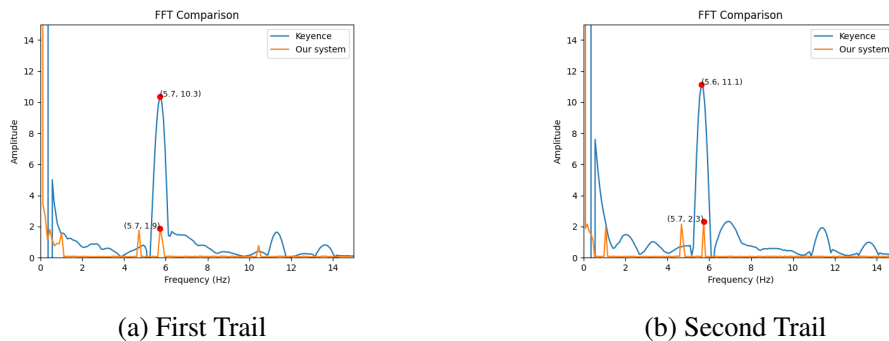


**Illustration 3–3 Fixed U-shaped part with middle width 15mm and 5 bars pressure.**

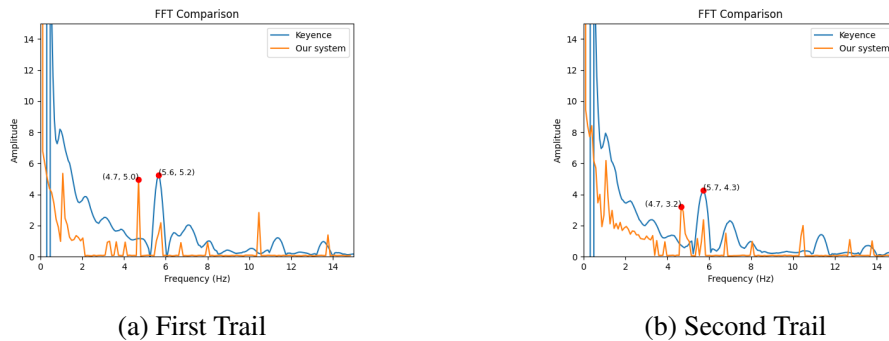
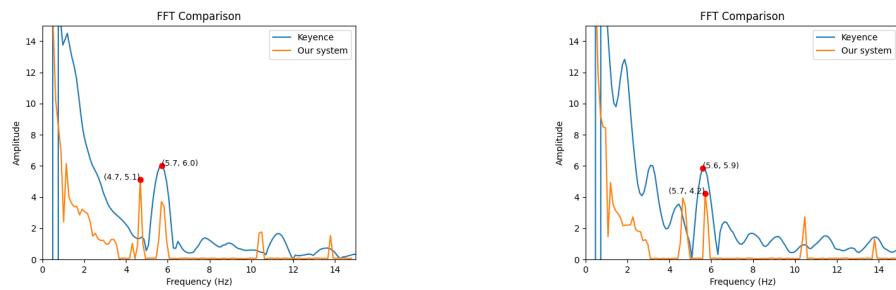


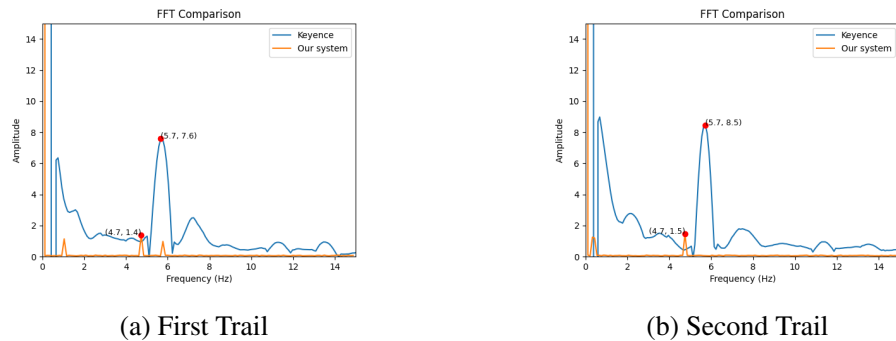
**Illustration 3–4 Fixed U-shaped part with middle width 5mm and 2 bars pressure.**



(a) First Trail

(b) Second Trail

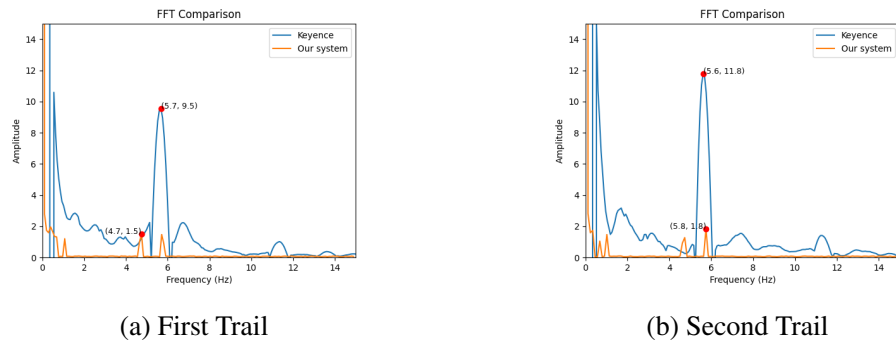
**Illustration 3–5 Fixed U-shaped part with middle width 5mm and 5 bars pressure.**



(a) First Trail

(b) Second Trail

**Illustration 3–6 Unfixed U-shaped part with middle width 15mm and 2 bars pressure.**



(a) First Trail

(b) Second Trail

**Illustration 3-7 Unfixed U-shaped part with middle width 15mm and 5 bars pressure.**

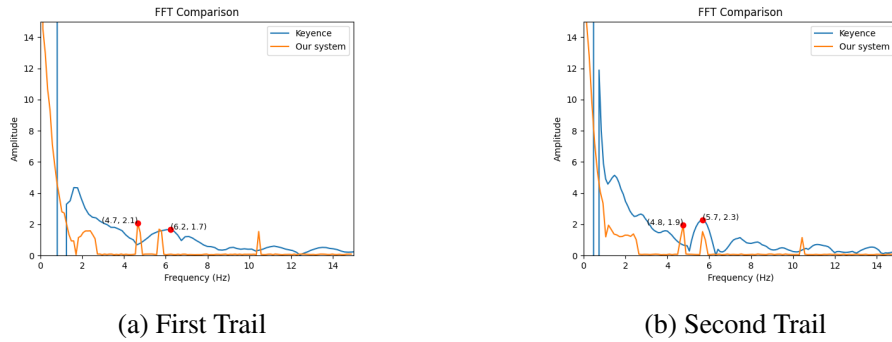


**Illustration 3–8 Unfixed U-shaped part with middle width 5mm and 2 bars pressure.**

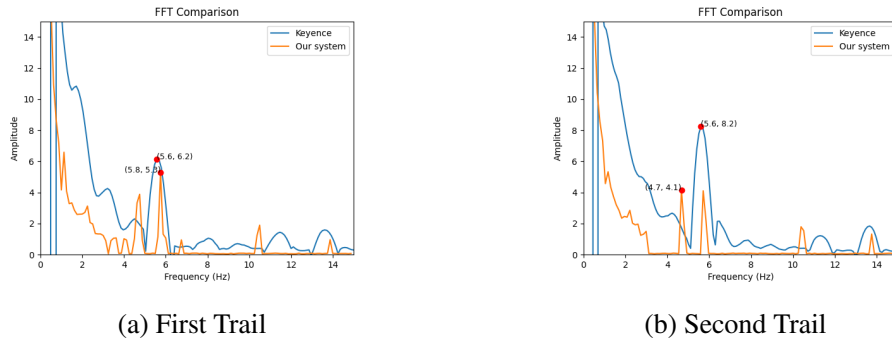


**Illustration 3–9 Unfixed U-shaped part with middle width 5mm and 5 bars pressure.**

### 3.3 Code

The code for User interface and Arduino programming can all be found in the Group24 public GitHub Repository (<https://github.com/FrankZhao-SJTU/VE450>).

# ANALYSIS OF VIBRATION-INDUCED MEASUREMENT INACCURACIES IN RIVETING PROCESSES

This project, sponsored by *Shanghai Systence*, focuses on optimizing riveting technology, specifically addressing inaccuracies caused by vibrations during the riveting process. Our investigation targets radial riveting technology, a commonly used technique in mechanical component assembly. Despite its prevalent usage, *Shanghai Systence* has faced challenges in quantitatively analyzing the riveting process, relying primarily on experiential knowledge and qualitative assessments. This traditional approach often falls short in addressing the complexities of the riveting process, leading to sub-optimal solutions, financial losses, wasted time, and diminished confidence in the company's problem-solving capabilities.

To overcome these challenges, we developed a cost-effective system designed to capture and analyze vibrations, providing actionable insights to improve product quality. Our research found that existing benchmarks in the market were either too expensive or limited to visualizing vibration patterns. In response, we designed a system that integrates both analysis results and vibration patterns into a single user interface, offering detailed and dense information to users. Collaborating with the sponsor company, we established several key requirements, including ease of use and accuracy. We used these requirements to define specific engineering specifications through a Quality Function Deployment (QFD) chart. Our solution incorporates a Keyence displacement laser sensor, a sensor amplifier, and an Arduino board for data acquisition, along with a PyQt-based software interface for visualization and analysis. These components were chosen for their ability to meet our specifications while staying within budget.

The system was validated through experiments, and while it successfully met most specifications, it faced challenges in detecting small vibrations due to hardware limitations. Future work will involve refining the system with more precise components. Overall, this project provides *Shanghai Systence* with a data-driven approach to refining the riveting process, potentially saving time and resources and enhancing market competitiveness. Despite some challenges, our work lays the groundwork for more accurate and efficient riveting processes, supporting *Shanghai Systence*'s operational excellence and future success.